Ageing and Rheology in Soft Materials

S. M. Fielding
Department of Physics and Astronomy, University of Edinburgh,
JCMB, King's Buildings,
Mayfield Road, Edinburgh, EH9 3JZ, GB.

P. Sollich
Department of Mathematics, King's College,
University of London, Strand, London, WC2R 2LS, GB.

M. E. Cates
Department of Physics and Astronomy, University of Edinburgh,
JCMB, King's Buildings,
Mayfield Road, Edinburgh, EH9 3JZ, GB.

December 14, 1999

Abstract

We study theoretically the role of ageing in the rheology of soft materials. We define several generalized rheological response functions suited to ageing samples (in which time translation invariance is lost). These are then used to study ageing effects within a simple scalar model (the "soft glassy rheology" or SGR model) whose constitutive equations relate shear stress to shear strain among a set of elastic elements, with distributed yield thresholds, undergoing activated dynamics governed by a "noise temperature", x. (Between yields, each element follows affinely the applied shear.) For $1 < x < 2$ there is a power-law fluid regime in which transients occur, but no ageing. For $x < 1$, the model has a macroscopic yield stress. So long as this yield stress is not exceeded, ageing occurs, with a sample's apparent relaxation time being of order its own age. The (age-dependent) linear viscoelastic loss modulus $G''(\omega, t)$ rises as frequency is *lowered*, but falls with age t, so as to always remain less than $G'(\omega, t)$ (which is nearly constant). Significant ageing is also predicted for the stress overshoot in nonlinear shear startup and for the creep compliance. Though obviously oversimplified, the SGR model may provide a valuable paradigm for the experimental and theoretical study of rheological ageing phenomena in soft solids.

1 Introduction

Many soft materials, such as foams, dense emulsions, pastes and slurries, display intriguing features in their low frequency shear rheology. In oscillatory shear, for example, their viscoelastic storage and loss moduli, $G'(\omega)$ and $G''(\omega)$, are often weak power laws of shear frequency (Mackley et al., 1994; Ketz et al., 1988; Khan et al., 1988; Mason et al., 1995; Panizza et al., 1996; Hoffmann and Rauscher,

1993; Mason and Weitz, 1995), while their nonlinear stress response σ to shear strain of constant rate $\dot{\gamma}$ is often fit to the form $\sigma = A + B\dot{\gamma}^n$ (known as the Herschel-Bulkley equation, or when $A = 0$, the power-law fluid) (Holdsworth, 1993; Dickinson, 1992; Barnes et al., 1989). The fact that such a broad family of soft materials exhibits similar rheological anomalies is suggestive of a common cause, and it has been argued that these anomalies are symptomatic of the generic presence in such materials of slow, glassy dynamics (Sollich et al., 1997; Sollich, 1998). Indeed, all the above materials share features of structural disorder and metastability: large energy barriers impede reorganization into states of lower free energy because this would require rearrangement of local structural units, such as the droplets in a dense emulsion. The term "soft glassy materials" (SGM's) has been proposed to describe such materials (Sollich et al., 1997; Sollich, 1998).

Glassy dynamics are often studied using hopping (trap) models, in which single particle degrees of freedom hop by an activated dynamics, in an uncorrelated manner, through a random free energy landscape (Bouchaud, 1992; Monthus and Bouchaud, 1996). By incorporating strain degrees of freedom into such a description, Sollich and coworkers (Sollich et al., 1997; Sollich, 1998) proposed a minimal model, called the "soft glassy rheology" (SGR) model, which appears to capture several of the rheological properties of SGM's, although (for simplicity) all the tensorial aspects of viscoelasticity are discarded. The model exhibits various regimes depending on a parameter x (discussed in more detail below) representing the "effective temperature" for the hopping process. When this is small ($x \leq 1$) the model exhibits a glass phase which shows some interesting properties above and beyond the power-law anomalies in viscoelasticity mentioned above. Specifically, the model shows *ageing behavior*: its properties depend on the elapsed time since a sample was prepared. This is because the population of traps visited never achieves a steady state; as time goes by, deeper and deeper traps dominate the behavior (a phenomenon known as "weak ergodicity breaking"). Broadly speaking, the system behaves as though its longest relaxation time is of order its own age.

The success of the SGR model in accounting for some of the generic flow properties of SGM's suggests that a detailed investigation of its ageing behavior, and the effect this has on rheology, is now worthwhile. Ageing has been intensively studied in the context of spin glasses (Bouchaud and Dean, 1995; Cugliandolo and Kurchan, 1995; Cugliandolo et al., 1997a; Bouchaud et al., 1998), although some of the earliest experimental investigations of it involved rheological studies of glassy polymers (Struik, 1978). But we know of no previous theoretical work that explores the link between ageing phenomena and rheological properties within an explicit constitutive model. A particular added motivation is that detailed experiments on rheological ageing, in a dense microgel suspension, are now underway (Cloître, 1999). Although various kinds of ageing effects are often observable experimentally in soft materials, they have rarely been reported in detail. Instead they tend to be regarded as unwanted obstacles to observing the "real" behavior of the system, and not in themselves worthy of study. But this may be illusory: ageing, when present, can form an integral part of a sample's rheological response. For example, the literature contains many reports of viscoelastic spectra in which the loss modulus $G''(\omega)$, while remaining less than

the (almost constant) storage modulus $G'(\omega)$ in a measured frequency window, appears to be increasing as frequency is lowered (see Fig. 1, bold lines). The usual explanation (e.g., Kossuth et al. (1999)) is that some unspecified relaxation process is occurring at a lower frequency still, giving a loss peak (dashed), whose true nature could be elucidated if only the frequency window was extended. This may often be the case, but an alternative explanation, based on our explicit calculations for the SGR model, is shown by the thin solid lines in Fig. 1, representing subsequent observations in a wider frequency window. No oscillatory measurement can probe a frequency far below the reciprocal of the sample's age; yet in ageing materials, it is the age itself which sets the relaxation time of whatever slow relaxations are present. Accordingly, the putative loss "peak" can never be observed and is, in fact, a complete figment of the imagination. Instead, a rising curve in $G''(\omega)$ at low frequencies will *always* be seen, but with an amplitude that decreases as the system gets older (typically ensuring that $G''(\omega)$ never exceeds $G'(\omega)$). Of course, we do not argue that all published spectra resembling those of Fig. 1 should be interpreted in this way; but we believe that many should be. A reluctance to acknowledge the role of ageing effects in parts of the rheological literature suggests that a full discussion of these could now be valuable. An exception has been in the literature on ageing in polymeric glasses, especially the monograph by Struik (1978): we return shortly to a brief comparison between that work and ours. In the area of structural glasses, ageing effects have also been investigated under the name of "structural relaxation" or "stabilization" (Scherer, 1986). They have been interpreted mainly using phenomenological "effective time theories", which are likewise discussed below.

The SGR model is simple enough to allow a fairly full exploration of the link between ageing and rheology. As well as providing some quantitative predictions of rheological ageing, this allows a broader discussion of the conceptual framework within which rheological data for ageing systems should be analysed and interpreted. This conceptual framework is broader than the SGR model itself; for example it is known that ageing concepts developed for spin-glass dynamics can also be applied to problems of domain-growth and coarsening (Bouchaud et al., 1998). Many soft solids, such as polydomain defect textures in ordered mesophases of copolymers or surfactants, may show ageing through such coarsening dynamics, or through glassy rearrangement of domains, or both. While the SGR model is intended to address only the second feature, the conceptual framework we present can allow for both mechanisms (in which case a superposition of ageing dynamics with different timescales may result; see Eq. (20) below).

Thus we begin in Secs. 2 and 3 by briefly introducing rheology and ageing respectively. Then in Sec. 4 we review the SGR model, and discuss the origin of its glass transition and the nature of the glass phase. We also briefly describe its rheology under non-ageing conditions; this is discussed fully elsewhere (Sollich et al., 1997; Sollich, 1998). In Sec. 5 we give a general discussion of ageing within the SGR model, which sets the stage for our new results for the linear and nonlinear rheological response of the SGR model in regimes where ageing cannot be neglected. The results for controlled strain conditions are presented and discussed in Sec. 6; those for controlled stress, in Sec. 7. We close in Sec. 8 with a brief summary and our conclusions.

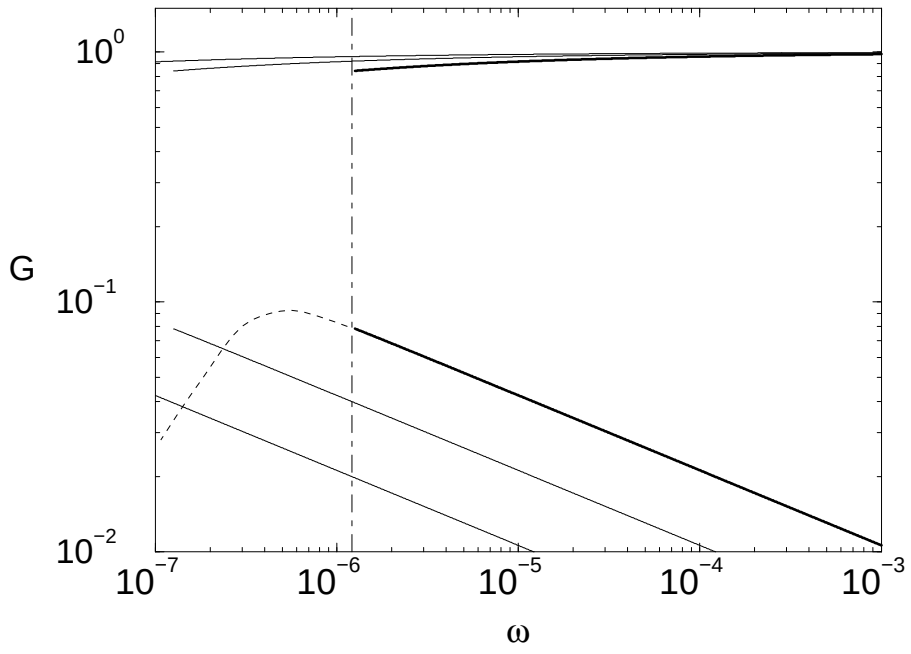

Figure 1: Sketch of ageing scenario for dynamic moduli G' (top) and G'' (bottom). Thick and thin solid lines: initial spectrum and two subsequent ones. Dashed: putative loss peak. Dot-dashed: limit to frequency window set initially by sample age. (In fact, the solid lines are calculated from the SGR model at noise temperature $x = 0.7$; see Sec. 6.1.2.)

We now discuss the connection between our work and that of Struik (1978) on polymeric glasses. Struik presented many experimental results for such systems, and gave a coherent qualitative explanation of their ageing in terms of a slow relaxation of the free volume in the system below the glass point. However, he did not propose a model constitutive equation for this or any other class of ageing material. He argued that the effective relaxation time of a system of age $t_{\rm w}$ (the 'waiting time' since sample preparation) varies as $\tau(t_{\rm w}) = t_{\rm w}^{\mu}\tau_0^{1-\mu}$, where τ_0 is a microscopic time and $\mu \simeq 1$; apart from this uniform rescaling of (all) the rheological relaxation time(s), the material properties are almost invariant in time. (This is his 'time waiting-time superposition' principle; we show below that the SGR model offers a concrete example of it, with $\mu = 1$.) We do not expect the SGR model, which makes no mention of the free-volume concept, to be particularly relevant to polymeric glasses; nonetheless, various points of contact with Struik's work are indicated below.

As mentioned above, ageing effects have also been studied in structural glasses; see Scherer (1986) for a comprehensive review, or Larson (1999) for a more recent summary. In this field, ageing is often referred to as structural relaxation or stabilization, and phenomenological theories have been developed to describe this process. A common ingredient is the assumption that deviations from time translation invariance during ageing can be captured by replacing time differences

$t - t'$ by differences in an "effective time" $\xi(t)$ (Hopkins, 1958)

$$t - t' \to \xi(t) - \xi(t'), \qquad \xi(t) = \int_0^t \frac{dt'}{\tau_{\rm r}(t')} \tag{1}$$

where $\tau_{\rm r}(t)$ is an age-dependent relaxation timescale. An additional hypothesis for the evolution of $\tau_{\rm r}(t)$ is then needed; a popular approach (Gardon and Narayanaswamy, 1970; Narayanaswamy, 1971) is to describe the current state of the sample in terms of a "fictive temperature" $T_{\rm f}$ and then to postulate coupled dynamical equations for $\tau(t)$ and $T_{\rm f}(t)$. This procedure appears to be particularly successful in rationalizing the properties of glasses subject to complicated temperature histories involving cooling and heating; for further details, we refer the reader to the book by Scherer (1986). In our general discussion of ageing in Sec. 3, we will see that the effective time $\xi(t)$ is closely related to what we will there call an ageing timescale. Note however that it is different from the effective time *interval* $Z(t, t')$ introduced below in the context of the SGR model.

2 Rheology

Here we review the basic principles of rheology. Unlike most in the literature, our formulation does not assume time translational invariance (TTI); parts of it may therefore be unfamiliar, even to rheologists. The formalism allows in principle an arbitrary dependence of the material properties on time; we defer to Sec. 3 a discussion of what form this dependence might take in materials which exhibit ageing effects (rather than other, more trivial time dependencies).

2.1 Constitutive Properties

In general, deformation can comprise volume changes, extensional strain, and shear strain; here we consider incompressible materials and assume that only shear strains arise. A system's shear stress $\sigma(t)$ then depends functionally on its strain rate history $\dot\gamma(t' < t)$, where $\dot\gamma$ is the strain rate. Conversely, $\gamma(t)$ can be expressed as a functional of the preceding stress history. A specification of either type is referred to as a *constitutive equation*. In general, of course, the constitutive equation is a relationship between stress and strain *tensors*; see Doi and Edwards (1986) for an introduction. We ignore the tensorial aspects here, because the model we describe later is too simple to address them.

2.2 Step Strain

A standard rheological test consists of suddenly straining a previously undeformed material by an amount γ_0. Suppose this to be done at time $t_{\rm w}$: then $\gamma(t) = \gamma_0 \Theta(t - t_{\rm w})$, where Θ is the usual step function. (For the moment, $t_{\rm w}$ is an arbitrary time label, but later we will take it as the time that the strain is applied, relative to the preparation of the sample in some prescribed state, at time zero.) The subsequent stress can be written

$$\sigma(t) = \gamma_0 G(t - t_{\rm w}, t_{\rm w}; \gamma_0) \tag{2}$$

thereby defining the step strain response, $G(t - t_{\rm w}, t_{\rm w}; \gamma_0)$.

2.3 Linearity

In the small deformation limit ($\gamma_0 \to 0$), a regime may exist for which σ is linearly related to γ_0:

$$\lim_{\gamma_0 \to 0} G(t - t_\mathrm{w}, t_\mathrm{w}; \gamma_0) = G(t - t_\mathrm{w}, t_\mathrm{w}) \tag{3}$$

The system's stress response is then linearly proportional to strain amplitude, in the sense that doubling the strain at all earlier times will cause the current stress to be doubled. Under these conditions, by decomposing the applied strain $\gamma(t)$ into a series of infinitesimal steps, one finds that

$$\sigma(t) = \int_{-\infty}^{t} G(t - t', t')\dot{\gamma}(t')\, dt' \tag{4}$$

which represents the most general (nontensorial) linearized constitutive equation. Note that there is no unique extension of this to the nonlinear case: the response to an arbitrary flow cannot in general be written solely in terms of $G(t-t_\mathrm{w}, t_\mathrm{w}; \gamma_0)$, although this is assumed for certain constitutive models (Bernstein et al., 1963).

If the material exhibits TTI, then $G(t-t_\mathrm{w}, t_\mathrm{w}; \gamma_0)$ can be written $G(t-t_\mathrm{w}; \gamma_0)$ – it depends only on the elapsed time since the step strain was imposed. Only by assuming *both* linearity and TTI do we obtain

$$\sigma(t) = \int_{-\infty}^{t} G(t - t')\dot{\gamma}(t')\, dt' \tag{5}$$

where $G(t-t_\mathrm{w})$ is the linear step-strain response as usually defined. In the steady state (constant $\dot{\gamma}$) one recovers:

$$\sigma = \dot{\gamma} \int_0^\infty G(t'')dt'' \tag{6}$$

The integral, whenever it exists, defines the material's zero-shear viscosity η. For many soft materials, however, $G(t)$ decays to zero so slowly that the integral diverges. In this case, there can be no regime of linear response in steady shear flow, although there may be a linear regime in, say, oscillatory shear.

2.4 Behavior of the Linear Response Function

The principle of causality demands that the response function $G(t - t_\mathrm{w}, t_\mathrm{w})$ is zero for times $t < t_\mathrm{w}$. At $t = t_\mathrm{w}$, G typically increases very rapidly (in effect discontinuously) to a value G_0, the instantaneous elastic modulus. Thereafter, $G(t-t_\mathrm{w}, t_\mathrm{w})$ is (almost always) a decaying function of its first argument. Specializing to the TTI case, we recall that for a purely Newtonian liquid of viscosity η, the function $G(t)$ approaches a delta function $\eta\delta(t)$, whereas an ideally Hookean elastic solid has $G(t) = G_0$. (Note that properly one should write $G(t) = G_0\Theta(t)$; the extra factor of $\Theta(t)$, implied by causality, is omitted here and below.)

Most real materials display intermediate behavior and are thus *viscoelastic*; for the soft materials of interest here, the timescale of the viscoelasticity is readily observable in rheological experiments. The simplest (TTI) example is the Maxwell fluid, which is solid-like at short times and liquid at longer ones, with

a simple exponential response function $G(t) = G_0 \exp(-t/\tau)$ connecting the two (so that $\eta = G_0\tau$). This behavior is seen in a few experimental systems (Cates and Candau, 1990), but $G(t)$ is usually not an exponential. In many materials it is possible to identify a longest relaxation time via $\tau_{\max}^{-1} = -\lim_{t\to\infty} \log G(t)/t$. However, in some important cases, for example that of a relaxation which decays asymptotically as a power law, $G(t) \sim t^{-y}$, the required limit does not exist, and the longest relaxation time is infinite.

2.5 Creep Compliance

Arguing along parallel lines to those developed above, we can write the strain response to a step stress $\sigma(t) = \sigma_0\Theta(t - t_{\rm w})$ as

$$\gamma(t) = \sigma_0 J(t - t_{\rm w}, t_{\rm w}; \sigma_0) \tag{7}$$

The linear creep compliance $J(t - t_{\rm w}, t_{\rm w})$ is then found by letting $\sigma_0 \to 0$ (assuming this limit exists).

For a system exhibiting TTI, the linear compliance reduces to a function of elapsed time, $J(t - t_{\rm w})$. (For a viscous liquid, an elastic solid, and a Maxwell material we have $J(t) = t/\eta$, $J(t) = 1/G_0$, and $J(t) = 1/G_0 + t/\eta$, respectively.) The zero-shear viscosity η can then be defined as the limiting ratio of stress to strain rate long after application of an infinitesimal step stress; it therefore obeys $\eta^{-1} = \lim_{t\to\infty} dJ(t)/dt$, which may be shown to be equivalent to (6) whenever the required limit exists (see also Sec. 2.7 below).

2.6 Viscoelastic Spectra

A common experiment is to apply a steady oscillatory strain and measure the resulting stress, or vice versa. For example, suppose that an ageing sample is prepared in a known state at time zero. The choice

$$\gamma(t) = \Theta(t - t_{\rm s}){\rm Re}\left[\gamma_0 e^{i(\phi+\omega t)}\right] \tag{8}$$

then describes an oscillatory flow started at time $t_{\rm s}$ after sample preparation, and continued up to (at least) the time t at which the stress is measured. For small enough γ_0, we can use the linear constitutive equation (4) to obtain

$$\begin{aligned} \sigma(t) &= {\rm Re}\left[\gamma_0 i\omega \int_{t_{\rm s}}^{t} e^{i(\phi+\omega t')} G(t - t', t')\, dt' + \gamma_0 e^{i(\phi+\omega t_{\rm s})} G(t - t_{\rm s}, t_{\rm s})\right] \\ &\equiv {\rm Re}\left[\gamma_0 e^{i(\phi+\omega t)} G^*(\omega, t, t_{\rm s})\right] \end{aligned} \tag{9}$$

where the second term in (9) accounts for any step strain arising at the switch-on time $t_{\rm s}$. This procedure defines a *time-varying* viscoelastic spectrum as

$$G^*(\omega, t, t_{\rm s}) = i\omega \int_{t_{\rm s}}^{t} e^{-i\omega(t-t')} G(t - t', t')\, dt' + e^{-i\omega(t-t_{\rm s})} G(t - t_{\rm s}, t_{\rm s}) \tag{10}$$

A similar compliance spectrum, $J^*(\omega, t, t_{\rm s})$ can be defined by exchanging stress and strain in this protocol.

Note that in principle, to identify by experiment the real and imaginary parts of G^* for given ω, t, t_s one would require the experiment to be repeated for two different phases ϕ (e.g., pure sine and cosine deformations). A more common procedure for TTI systems is to maintain the oscillatory strain over many cycles and record the "steady state" amplitude and phase response of the stress. However, in systems without TTI this will only give a unique result when material properties vary slowly enough; whenever it does, it will coincide with (10).

Since it depends on two time arguments as well as frequency, $G^*(\omega, t, t_s)$ is a cumbersome object. However, simplifications arise in the limit $\omega(t - t_s) \gg 1$.

2.6.1 Viscoelastic spectra in TTI case

In the TTI case, where $G^*(\omega, t, t_s)$ depends only on the time interval $t - t_s$, the further condition $\omega(t - t_s) \gg 1$ can be used to eliminate simple transients. The stress then settles to a simple harmonic function of time and we can write $\sigma(t) = \mathrm{Re}\,[G^*(\omega)\gamma(t)]$ where[1]

$$G^*(\omega) = i\omega \int_0^\infty e^{-i\omega t} G(t)\, dt \tag{11}$$

Traditionally one writes $G^*(\omega) = G'(\omega) + iG''(\omega)$ where G', G'', the storage and loss moduli, give the in-phase (elastic) and out-of-phase (dissipative) response to an applied strain.

Clearly one can reach an identical steady state by applying a small amplitude oscillatory stress and measuring the resulting strain. This defines, for the TTI case, a complex compliance $J^*(\omega)$ via $\gamma(t) = \mathrm{Re}\,[J^*(\omega)\sigma(t)]$, which is just the reciprocal of $G^*(\omega)$. But by an argument similar to that given above for (11) one also has $J^*(\omega) = i\omega \int_0^\infty e^{-i\omega t} J(t)\, dt$. Hence, within the linear response regime of a system with TTI, knowledge of any one of $G(t), J(t), G^*(\omega), J^*(\omega)$ is enough to determine the other three.

2.6.2 Viscoelastic Spectra without TTI

A similar set of simplifications are certainly not guaranteed in the absence of TTI. However, the transient dependence on t_s *may* become negligible when $\omega(t - t_s) \gg 1$, in which case we have

$$G^*(\omega, t, t_s) \to G^*(\omega, t) \tag{12}$$

giving a viscoelastic spectrum that depends only on the measurement time t. If, in addition, the time evolution of the underlying material properties is negligible on the timescale of one oscillation, then $G^*(\omega, t)$ *may* obey the relation

$$G^*(\omega, t) = i\omega \int_0^\infty e^{-i\omega t'} G(t', t)\, dt' \tag{13}$$

Similarly, for $\omega(t - t_s) \gg 1$ the compliance spectrum *may* become t_s-independent, $J^*(\omega, t, t_s) \to J^*(\omega, t)$, and *may* be related to the step stress response via

$$J^*(\omega, t) = i\omega \int_0^\infty e^{-i\omega t'} J(t', t)\, dt' \tag{14}$$

[1]Note that if $G(t)$ has a non-decaying contribution $G(t \to \infty) > 0$, the form $G^*(\omega) = G(0) + \int_0^\infty e^{-i\omega t} G'(t)\, dt$, derived from (9) by integration by parts, should be used instead of (11).

Finally, $G^*(\omega,t)$ and $J^*(\omega,t)$ *may* obey the usual reciprocal relation $G^*(\omega,t) = 1/J^*(\omega,t)$. Indeed, we shall find that all the above simplifying relationships are true for the SGR model (subject to an additional requirement that $\omega t_s \gg 1$; see Sec. 6.1.2 below). As discussed at the end of Sec. 3, they may also hold more generally for systems with "weak long term memory". However, we do not have a proof for this; experimenters and theorists alike should beware that, for systems without TTI, such textbook relationships between the oscillatory and step strain response functions cannot be assumed, but should be verified, for each system studied. This *prima facie* breakdown of conventional linear viscoelastic relationships in ageing systems was emphasized by Struik (1978), though he argued that they are recovered in sufficiently 'short-time' measurements. It does not (as Struik seems to suggest) extend necessarily to breakdown of linear superposition itself, which survives in the form of (4). In fact, breakdown of TTI is a quite separate issue from nonlinearity; neither implies the other.

2.7 Steady State Response: The Flow Curve

Consider now the ultimate state of a material, with TTI, long after an infinitesimal step stress of amplitude σ_0 has been applied. The ultimate deformation may involve a limiting strain $\gamma = \sigma_0 J(t \to \infty)$, in which case the steady state elastic modulus is $G_\infty = \sigma_0/\gamma$. Alternatively, it may involve a limiting strain rate, in which case the zero-shear viscosity is $\eta = \sigma_0/\dot{\gamma}$. However, neither outcome need occur. If, for example, one has "power law creep", *i.e.*, $J(t) \sim t^y$ with $0 < y < 1$, the material has both zero modulus (infinite compliance) and infinite viscosity in steady state. (This requires that $\tau_{\max}$ is infinite.)

What if the stress amplitude is larger than infinitesimal? The ultimate steady state can again be that of a solid, a liquid, or something in between. When a liquid-like response is recovered, it is conventional to measure the "flow curve", or steady state relationship between stress and strain rate: $\sigma_{ss} = \sigma(\dot{\gamma})$. In many materials, the following limit, called the yield stress

$$\sigma(\dot{\gamma} \to 0) = \sigma_y \tag{15}$$

is nonzero. (The experimental existence of a true yield stress, in this sense, is debatable (Barnes et al., 1989), though behavior closely approaching it is often reported.)

The presence of nonzero yield stress does not necessarily imply a finite Hookean modulus G_∞: for $\sigma < \sigma_y$, the material could creep forever, but at an ever decreasing rate. (Alternatively, it could reach a steady strain γ that is not linear in σ even as $\sigma \to 0$.) Nor does the *absence* of a finite yield stress imply a finite viscosity; a counterexample is the power law fluid, for which $\sigma \sim \dot{\gamma}^p$. This has $\sigma_y = 0$ but, for $p < 1$, infinite viscosity $\eta = \lim_{\dot{\gamma}\to 0} \sigma(\dot{\gamma})/\dot{\gamma}$.

What about the flow curve for materials without TTI? For these, no meaningful definition of "steady state response" exists in general. However, in the SGR model considered below, TTI is restored for nonzero $\dot{\gamma}$ (Sollich et al., 1997; Sollich, 1998), and this may be generic for certain types of ageing (Sollich et al., 1997; Sollich, 1998; Bouchaud and Dean, 1995; Kurchan, 1998). If so the flow

curve, including the value of the yield stress σ_y (but *not* the behavior for $\sigma < \sigma_y$) remains well-defined.

3 Ageing

So far, we have set up a general framework for describing the rheological properties of systems without TTI. Time translation invariance can be broken, in a trivial sense, by the transients that any system exhibits during equilibration. We now consider how such transients can be distinguished from ageing proper. To focus the discussion, we consider the linear step strain response function $G(t - t_w, t_w)$. The other response functions introduced above can be treated similarly. We define ageing (of the step strain response) as the property that *a significant part of the stress relaxation takes place on timescales that grow with the age t_w of the system.* If ageing is present, then in order to see the full stress relaxation we need to allow the time t at which we observe the stress to be much larger than the time t_w at which the step strain has been applied. Formally, we need to consider

$$\lim_{t\to\infty} G(t - t_w, t_w) \tag{16}$$

at *fixed* t_w. On the other hand, if there is no ageing, then the full stress relaxation is "visible" on finite timescales. This means that as long as $\Delta t = t - t_w$ is large enough, we observe the full stress relaxation whatever the age t_w of the system at the time when the strain was applied. Formally, we can take t_w to infinity first, and then make Δt large, which amounts to considering

$$\lim_{\Delta t\to\infty} \lim_{t_w\to\infty} G(\Delta t, t_w). \tag{17}$$

In the absence of ageing, the two ways (16) and (17) of measuring the final extent of stress relaxation are equivalent, and we have

$$\lim_{t\to\infty} G(t - t_w, t_w) = \lim_{\Delta t\to\infty} \lim_{t_w\to\infty} G(\Delta t, t_w). \tag{18}$$

If the system ages, on the other hand, this equality will not hold: the right-hand side allows only for the decay of stress by relaxation modes whose timescale does not diverge with the age of the system, and thus attains a limit which includes elastic contributions from all modes that do have age-related timescales. It will be different from the left-hand side, which allows for relaxation processes occurring on all timescales, and thus attains a limit in which only completely non-decaying modes contribute. We therefore adopt the definition that a systems *ages* if at least one of its response functions violates (18). By contrast, we refer to deviations from TTI in other systems (for which all significant relaxation processes can essentially be observed on finite timescales) as *transients*. We discuss this point further in the context of the SGR model in Sec. 6.1.1.

Systems that violate (18) are said to have "long term memory" (Cugliandolo and Kurchan, 1995; Bouchaud et al., 1998; Cugliandolo and Kurchan, 1993). They can be further subdivided according to the strength of this memory. To illustrate this distinction, imagine applying a (small) step strain to a system at

time t_0 and switching it off again at some later time t_1. The corresponding stress at time $t > t_1$ is proportional to $G(t-t_0,t_0) - G(t-t_1,t_1)$. If this decays to zero at large times t, that is, if

$$\lim_{t\to\infty} [G(t-t_0,t_0) - G(t-t_1,t_1)] = 0 \tag{19}$$

[and (18) is violated] then we say that the system has "weak long term memory", otherwise it has "strong long term memory".[2] Although the weakness condition (19) does not hold for all response functions in all ageing systems, it seems rather natural to expect it, in the rheological context, for most materials of interest. Indeed, a system with *weak* long term memory eventually forgets any perturbation that was only applied to it during a finite period. Thus, the treatment of a sample directly after it has been prepared (by loading it into the rheometer, preshearing, etc.) will not have a strong impact on the age-dependence of its rheological properties. This is the usual experience, and is obviously needed for the reproducibility of experiments results; likewise, it means that one can hope to make theoretical predictions which are not sensitive to minute details of the sample preparation. For the SGR model, any long term memory is indeed weak (as shown in Sec. 6.1.1 below); we consider this an attractive feature. Note in any case that a rheological theory for systems with strong long term memory might look very different from the SGR model.

We have defined ageing as the property that a significant part of the stress relaxation $G(t-t_\mathrm{w},t_\mathrm{w})$ takes place on timescales that grow with the age t_w of the system. In the simplest case, there is only one such growing timescale, proportional to the age of the system itself. The (ageing part of the) stress relaxation then becomes a function of the scaled time difference $(t-t_\mathrm{w})/t_\mathrm{w}$. We will encounter such simple ageing behavior in the glass phase of the SGR model, which is discussed below. More complicated ageing scenarios are possible, however: There may be several timescales that grow differently with the age of the system. This can be represented as

$$G(t-t_\mathrm{w},t_\mathrm{w}) = \sum_i \mathcal{G}_i\left[h_i(t)/h_i(t_\mathrm{w})\right] \tag{20}$$

where the functions $h_i(t)$ define the different diverging timescales. If there is only a single term in the sum, with $h(t) = t$, then the simplest ageing scenario (shown by the SGR model) is recovered. To see that (20) also includes TTI and intermediate ageing scenarios, it is useful to rewrite it in the form

$$G(t-t_\mathrm{w},t_\mathrm{w}) = \sum_i \tilde{\mathcal{G}}_i\left[\xi_i(t) - \xi_i(t_\mathrm{w})\right] \tag{21}$$

where $\xi_i = \ln h_i$ and $\tilde{\mathcal{G}}_i(\ln h) = \mathcal{G}_i(h)$. For $\xi(t) = t/\tau_0$, corresponding to $h(t) = \exp(t/\tau_0)$ (where τ_0 is a microscopic time), one has TTI. More generally, $\xi(t) =$

[2] There is a slight subtlety with the definition of long term memory for the linear step stress response. Eq. (19), applied literally to $J(t-t_\mathrm{w},t_\mathrm{w})$, suggests that even a Newtonian fluid with $J(t-t_\mathrm{w},t_\mathrm{w}) \sim t - t_\mathrm{w}$ has strong long term memory, because its strain "remembers" stress applications in the arbitrarily distant past. This is clearly undesirable as a definition. The problem can be cured by "regularizing" the step stress response: one simply considers the material in question "in parallel" with an elastic spring with infinitesimal modulus.

$(t/\tau_0)^{1-\mu}$ interpolates between TTI for $\mu = 0$ and simple ageing ($h(t) = t$, $\xi(t) \sim \ln t$) for $\mu \to 1$. In the regime of short time differences ($t - t_\mathrm{w} \ll t_\mathrm{w}$), one then finds that the response function depends on

$$\xi(t) - \xi(t_\mathrm{w}) = \frac{1-\mu}{\tau_0^{1-\mu}} \frac{t - t_\mathrm{w}}{t_\mathrm{w}^\mu} \; . \tag{22}$$

Ignoring the irrelevant prefactor, one thus recovers Struik's general 'time waiting-time superposition principle' (Struik, 1978).

Eq. (21) provides an interesting point of contact with the effective time theories for ageing effects that we mentioned briefly in the introduction. In fact, if we define an age-dependent relaxation timescale by

$$\frac{1}{\tau_\mathrm{r}} = \frac{d\xi}{dt} = \frac{d \ln h}{dt}$$

then each term in the sum over i in (21) has exactly the form postulated by the effectime time approach (compare (1)). For simple ageing, we have $h(t) = t$ and $\xi(t) = \ln t$, giving $\tau_\mathrm{r}(t) = t$ as expected: The relaxation timescale is proportional to the age of the system. For TTI, on the other hand, $\xi(t) = t/\tau_0$ and so $\tau_\mathrm{r}(t) = \tau_0$ is independent of time, again as expected. The form $\xi(t) = (t/\tau_0)^{1-\mu}$ interpolates between these limits, with $\tau_\mathrm{r}(t) \sim t^\mu$. In general, we can interpret (21) as a generalization of the effective time approach to the case where different effective times $\xi_i(t)$ are needed to describe the ageing behavior of the system. This is not merely a phenomenological model, however: Cugliandolo and Kurchan (1994) have shown under fairly mild assumptions that (20) is the most general representation of the asymptotic behavior of step response and correlation functions in systems with weak long term memory.

To avoid misunderstandings, we emphasize that (21) only describes how the stress relaxation of the system depends on its age t_w at the time when a step strain is applied. It does not determine the "shape" of the relaxation, which is encoded by the functions $\tilde{\mathcal{G}}_i$. In ageing systems, one expects a broad relaxation time spectrum centred around the timescale τ_r, corresponding to nonexponential $\tilde{\mathcal{G}}$. A popular representation is the stretched exponential $\tilde{\mathcal{G}} \sim \exp(-\xi^\beta)$, which for $\xi(t) = (t/\tau_0)^{1-\mu}$ would correspond to a stress relaxation of the form

$$G(t - t_\mathrm{w}, t_\mathrm{w}) \sim \exp\left[-\frac{(t^{1-\mu} - t_\mathrm{w}^{1-\mu})^\beta}{\tau_0^{\beta(1-\mu)}} \right]$$

Looking back at (22), we see that this would represent a crossover from a stretched exponential in $t - t_\mathrm{w}$ with stretching exponent β for short times $t - t_\mathrm{w} \ll t_\mathrm{w}$ to one with stretching exponent $\beta(1-\mu)$ for long times.

Finally, let us return to the status of Eqs. (12,13,14). (These concern the lack of t_s-dependence in $G^*(\omega, t, t_\mathrm{s})$, the Fourier relationship between frequency and real-time spectra, and the reciprocity between G^* and J^*.) As stated in Sec. 2.6.2 these equations have no general validity for systems without TTI. Indeed, one can easily construct theoretical model systems with *strong* long term memory which violate them. On the other hand, we speculate that systems with *weak* long term memory will generically have the properties (12,13,14).

4 The SGR model

The phenomenological SGR model captures many of the observed rheological properties of soft metastable materials, such as foams, emulsions, slurries and pastes (Mackley et al., 1994; Ketz et al., 1988; Khan et al., 1988; Mason et al., 1995; Panizza et al., 1996; Hoffmann and Rauscher, 1993; Mason and Weitz, 1995). It is based upon Bouchaud's trap model of glassy dynamics, with the addition of strain degrees of freedom, and the replacement of the thermodynamic temperature by an effective (noise) temperature. It incorporates only those characteristics deemed common to all soft glassy materials (SGM's), namely structural disorder and metastability. We now review its essential features.

We conceptually divide a macroscopic sample of SGM into many mesoscopic elements. By mesoscopic we mean large enough such that the continuum variables of strain and stress still apply for deformations on the elemental scale, and small enough that any macroscopic sample contains enough elements to allow the computation of meaningful "averages over elements". We then assign to each element a local strain l, and corresponding stress kl, which describe deformation away from some local position of unstressed equilibrium relative to neighbouring elements. The macroscopic stress of the sample as a whole is defined to be $\langle kl \rangle$, where $\langle\,\rangle$ denotes averaging over elements. Note that, for simplicity, (shear-) stress and strain are treated as scalar properties. The model therefore does not predict, or allow for, the various normal stresses which can arise in real materials undergoing nonlinear shear (Doi and Edwards, 1986).

For a newly prepared, undeformed sample, we make the simplest assumption that $l = 0$ for each element. (Physically, of course, $\langle l \rangle = 0$ would be sufficient and is indeed more plausible.) The subsequent application of a macroscopic strain at rate $\dot{\gamma}$ causes each element to strain relative to its local equilibrium state and acquire a non-zero l. For a given element, this continues up to some maximal strain $l_{\rm y}$, at which point that element yields, and rearranges into a new configuration of local equilibrium with local strain $l = 0$. This ignores possible "frustration" effects: an element may not be able to relax to a fully unstrained equilibrium position due to interactions with neighbouring elements. (Such effects can be incorporated into the model, but are not expected to affect the results in a qualitative way (Sollich, 1998).) Under continued macroscopic straining, the yielded element now strains relative to its new equilibrium, until it yields again; its local strain (and stress) therefore exhibits a saw-tooth dependence upon time.

The simplest assumption to make for the behavior between yields is that $\dot{\gamma} = \dot{l}$: the material deformation is locally affine (Doi and Edwards, 1986). Yield events apart, therefore, the SGR model behaves as an elastic solid of spring constant k. Yields confer a degree of liquidity by providing a mechanism of stress relaxation.

Although we have introduced yielding as a purely strain-induced phenomenon, we in fact model it as an "activated" process (Sollich et al., 1997; Sollich, 1998). We assume that an element of yield energy $E = \frac{1}{2}kl_{\rm y}^2$, strained by an amount l, has a certain probability for yielding in a unit time interval. We write this rate as τ^{-1}, where the characteristic yield time

$$\tau = \tau_0 \exp\left[(E - \frac{1}{2}kl^2)/x\right] \tag{23}$$

is taken to be the product of an attempt time and an activation factor which is thermal in form. This captures the strain-induced processes described above since any element strained beyond its yield point will yield exponentially quickly; but it also allows even totally unstrained elements to yield by a process of activation over the energy barrier E. These activation events mimic, within our simplified model, nonlinear couplings to other elements (the barrier heights depend on the surroundings, which are altered by yield events elsewhere). A more complete model would treat these couplings explicitly. However, in the SGR model, which does not, x is regarded as an effective "noise" temperature to model the process. (Alternatively, we can think of x as the typical *energy* available for an activated processes. We use units in which the Boltzmann constant $k_B = 1$ throughout, so there is no need to distinguish between these two interpretations of x as either a temperature or an energy.) Because the energy barriers are (for typical foams, emulsions, etc.) large compared to the thermal energy $k_B T$, so are the energy changes caused by these nonlinear couplings, and so to mimic these, one expects to need x of order the mean barrier height $\langle E \rangle$. Whether it is fully consistent to have a noise temperature $x \gg k_B T$ is a debatable feature of the model (Sollich et al., 1997; Sollich, 1998); however, we think the results are sufficiently interesting to justify careful study of the model despite any uncertainty over its interpretation. (It is also intriguing to note that similar "macroscopic" effective temperatures, which remain nonzero even for $k_B T \to 0$, have recently been found in other theories of out-of-equilibrium systems with slow dynamics (Kurchan, 1998; Cugliandolo et al., 1997b).) Note that the SGR model treats "noise-induced" yield events (where the strain is much below the yield strain $l_{\rm y}$, *i.e.*, where $\frac{1}{2}kl^2 \ll E$) and "strain-induced" yield events (where $\frac{1}{2}kl^2 \approx E$) in a unified fashion. We will nevertheless find it useful below to distinguish between these two classes occasionally.

The disorder inherent to SGM's is captured by assuming that each element of a macroscopic sample has a different yield energy: a freshly yielded element is assigned a new yield energy selected at random from a "prior" distribution $\rho(E)$. This suggests the following alternative view of the dynamics of the SGR model, which is represented graphically in Fig. 2. Each material element of a SGM can be likened to a particle moving in a landscape of quadratic potential wells or "traps" of depth E. The depths of different traps are uncorrelated with each other and distributed according to $\rho(E)$. The bottom of each trap corresponds to the unstrained state $l = 0$; in straining an element by an amount l, we then effectively drag its representative particle a distance $\frac{1}{2}kl^2$ up the sides of the trap, and reduce the effective yield barrier height ($E \to E - \frac{1}{2}kl^2$). Once the particle has got sufficiently close to the top of its trap ($E - \frac{1}{2}kl^2 \approx x$), it can hop by activated dynamics to the bottom of another one. This process corresponds to the yielding of the associated material element. In the following, we shall use the terminology of both the "element picture" and the "particle picture" as appropriate. Thus, we will refer to $\tau = \tau_0 \exp\left[(E - \frac{1}{2}kl^2)/x\right]$ as either the yield or relaxation time of an element, or as the lifetime of a (particle in) a trap or element. The inverse of τ is the rate at which an element yields/relaxes or a particle hops. However, we normally reserve the term 'yield rate' or 'hopping

rate' for the *average* of these rates over the whole system, *i.e.*, over all elements or particles. This quantity is denoted Y and will occur frequently below.

A specific choice of $\rho(E)$ is now made: $\rho(E) = (1/x_g)\exp(-E/x_g)$, where $x_g = \langle E \rangle$ is the mean height of a barrier chosen from the prior distribution $\rho(E)$. As shown by Bouchaud (1992), the exponential distribution, combined with the assumed thermal form for the activated hopping, is sufficient to give a glass transition in the model. The transition is at $x = x_g$ and divides the glass phase ($x \leq x_g$), in which weak ergodicity breaking occurs, from a more normal phase ($x > x_g$). In the glass phase, the Boltzmann distribution (which is the only possible steady state for activated hopping dynamics, in the absence of strain),

$$P_{\rm eq}(E) \propto \rho(E)\exp(E/x) \tag{24}$$

is not normalizable: thus there is no steady state, and the system must age with time. (The converse applies for $x > x_g$: there is then a unique equilibrium state, which is approached at long times. Hence ageing does not occur, though there may be transients in the approach to equilibrium.) Apart from our use of an effective temperature x, the only modification to Bouchaud's original model of glasses lies in our introduction of dynamics within traps coupled to strain.

It may appear suspicious that, to obtain a glass transition at all, an exponential form of $\rho(E)$ is required (though strictly, only for large E (Bouchaud, 1992)). In reality, however, the glass transition is certainly a collective phenomenon: the remarkable achievement of Bouchaud's model is to represent this transition within what is, essentially, a single-particle description. Thus the chosen "activated" form for the particle hopping rates, and the exponential form of the trap depth distribution, should not be seen as two independent (and doubtful) physical assumptions, but viewed jointly as a tactic that allows glassy dynamics to be modelled in the simplest possible way (Sollich et al., 1997; Sollich, 1998).

From now on, without loss of generality, we choose units so that both $x_g = k = 1$. This means that the strain variable l is defined such that an element, drawn at random from the prior distribution, will yield at strains of order one. Since the actual value of the strain variable can be rescaled within the model (the difference being absorbed in a shift of k), this is purely a matter of convention. But our choice should be borne in mind when interpreting our results for nonlinear strains, given below: where strains "of order unity" arise, these are in fact of order some yield strain $l_{\rm y}$, which the model does not specify, but which may in reality be a few percent or less. In addition we choose by convention $\tau_0 = 1$; the timescale in the SGR model is scaled by the mesoscopic "attempt time" for the activated dynamics. The low frequency limit, which is the main regime of interest, is then defined by $\omega\tau_0 = \omega \ll 1$. Note that, with our choice of units, $\langle E \rangle = 1$ so that we expect the interesting physics to involve $x \simeq 1$.

4.1 Constitutive Equation

The SGR model is exactly solved by two coupled constitutive equations (Sollich, 1998), the first of which expresses strain as an integral over stress history, while the second embodies the conservation of probability. We assume that the sample is prepared (in a known initial state of zero stress and strain) at time zero and

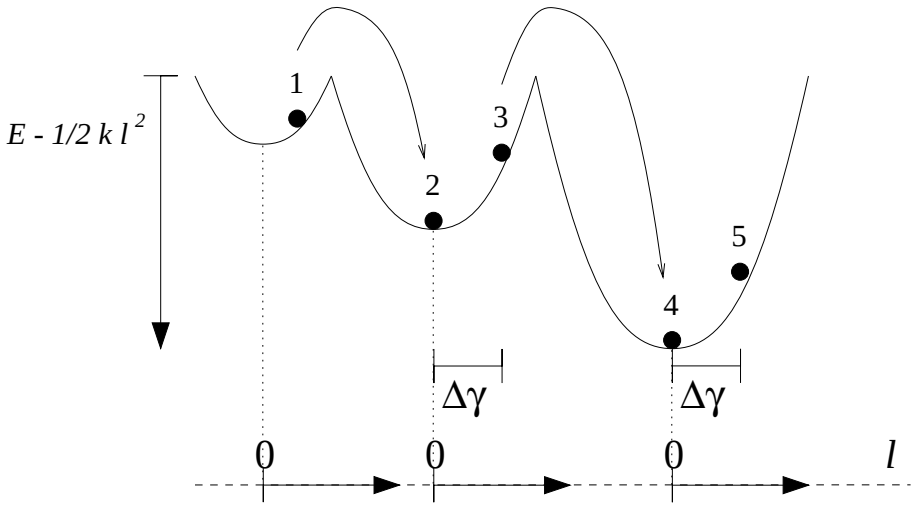

Figure 2: Dynamics of the SGR model. A representative particle (1) may hop out of its trap by activated hopping ($1 \to 2$). It enters the new trap in a state of zero local strain ($l = 0$); application of strain $\Delta\gamma$ raises its energy ($2 \to 3$) making a subsequent hop ($3 \to 4$) more likely. Note that the horizontal position of the quadratic potential wells (traps) is arbitrary; each has its own independent zero for the scale of the local strain l.

that a time dependent macroscopic strain $\gamma(t)$ is applied thereafter, so $\gamma(t) = 0$ for $t \leq 0$. The constitutive equations are then

$$\sigma(t) = \gamma(t)G_0(Z(t,0)) + \int_0^t \left[\gamma(t) - \gamma(t')\right] Y(t')G_\rho(Z(t,t'))dt' \tag{25}$$

$$1 = G_0(Z(t,0)) + \int_0^t Y(t')G_\rho(Z(t,t'))dt' \tag{26}$$

In these equations

$$Z(t,t') = \int_{t'}^t \exp\left(\left[\gamma(t'') - \gamma(t')\right]^2 / 2x\right) dt'' \tag{27}$$

while $Y(t')$ is the average yield rate rate at time t'. The functions $G_\rho(Z)$ and $G_0(Z)$ obey

$$G_\rho(Z) = \int_0^\infty \rho(E) \exp\left(-Ze^{-E/x}\right) dE \tag{28}$$

$$G_0(Z) = \int_0^\infty P_0(E) \exp\left(-Ze^{-E/x}\right) dE \tag{29}$$

where $P_0(E)$ is the probability distribution for the yield energies (or trap depths) in the initial state of preparation of the sample at time $t = 0$. We return below (Sec. 5.1) to the issue of how to choose this initial state.

These equations can be understood by viewing yielding as a "birth and death" process: each time an element yields it dies and is reborn with zero stress, and with a yield energy selected randomly from the prior distribution

$\rho(E)$. The (average) yield rate rate at time t' is $Y(t')$; the birth rate at time t' of elements of yield energy E is therefore $Y(t')\rho(E)$. The proportion of these which survive without yielding until time t is found as $\exp\left[-Z(t,t')/\tau(E)\right]$ where $\tau(E) = \exp(E/x)$ is the (mean) lifetime that an unstrained element of yield energy E would have. The expression (27) for $Z(t,t')$ reflects the fact that an element that last yielded at time t' and has a yield energy E will have a yield rate of $\tau(E)^{-1}\exp\left(\left[\gamma(t'')-\gamma(t')\right]^2/2x\right)$ at time t''. Here the exponential factor accounts for the lowering of the yield barrier by strain applied since the element last yielded (see Fig. 2). Note that this factor is unity under conditions where the local strain is everywhere negligible, in which case $Z(t,t') \to t - t'$. More generally, $Z(t,t')$ can be thought of as an effective time interval measured on an "internal clock" within an element, which allows for the effect of local strain on its yield rate, by speeding up the clock. This speeding up effect, which describes strain-induced yielding, is the only source of nonlinearity within the SGR model. Note that this nonlinearity is not of the simple form of a strain-dependent effective time (see, e.g., (Hodge, 1995) and references therein), as comparison of (1) with (27) might at first suggest: The integrand in (27) is not just a function of the integration variable t'', but also of the inital time t'. More importantly, the nonlinear variation of $Z(t,t')$ with strain feeds back into the average yield rate $Y(t)$, and from there into the stress $\sigma(t)$, in a way that is nonlocal in time. This precludes any simple "effective time" interpretation of the SGR model as a whole: it does *not* obey (1).

According to the above arguments, the number of elements of yield energy E, present at time t, which were last reborn at time t' is

$$P(E,t,t') = Y(t')\rho(E)\exp\left[-Z(t,t')/\tau(E)\right] \tag{30}$$

Such elements each carry a local strain $\gamma(t) - \gamma(t')$ and so the net contribution they make to the stress at time t is

$$s(E,t,t') = \left[\gamma(t) - \gamma(t')\right] Y(t')\rho(E)\exp\left[-Z(t,t')/\tau(E)\right] \tag{31}$$

Integrating these expressions over t' from 0 to t and adding terms representing the contribution from elements which have survived from $t = 0$ without yielding at all, we get respectively the number $P(E,t)dE$ of elements at time t with yield energies between E and $E + dE$:

$$P(E,t) = P_0(E)\exp\left[-Z(t,0)e^{-E/x}\right] + \int_0^t P(E,t,t')dt' \tag{32}$$

and the corresponding stress contribution $s(E,t)dE$ at time t from such elements:

$$s(E,t) = \gamma(t)P_0(E)\exp\left[-Z(t,0)e^{-E/x}\right] + \int_0^t s(E,t,t')dt' \tag{33}$$

Integrating (32) and (33) over all yield energies E, we finally recover our constitutive equations (25) and (26) respectively. Below we will return to $P(E,t)$ and $s(E,t)$, which will sometimes be expressed instead as a function of the lifetime $\tau(E) = \exp(E/x)$ of an unstrained element with yield energy E, so that

$P(\tau,t)d\tau = P(E,t)dE$ and likewise for s. Note that, because $E \geq 0$, these distributions are nonzero only for $\tau \geq 1$. We will not write this restriction explicitly below.

Finally, the following alternative form of the first constitutive equation (25) is sometimes useful:

$$\sigma(t) = \gamma(t) - \int_0^t \gamma(t')Y(t')G_\rho(Z(t,t'))dt' \tag{34}$$

This is obtained by substituting (26) into (25).

4.2 Rheological Properties of the SGR Model

Solution of the constitutive equations (25, 26) is relatively straightforward under conditions where TTI applies. Here we recall the main results thereby obtained (Sollich et al., 1997; Sollich, 1998).

4.2.1 Linear Spectra

A regime of linear rheological response arises whenever the effects of strain on the effective time interval $Z(t,t')$ is small. This requires that the local strains in each element remain small; in oscillatory shear, where $\gamma(t) = \gamma_0 e^{i\omega t}$, this is satisfied at low enough strain amplitudes γ_0 for any finite frequency ω. (The same is not true in steady shear flow; we return to this in Sec. 4.2.2 below.) In the linear regime, the model's internal dynamics are independent of the imposed deformation: the elements' lifetimes are, to order γ_0, strain-independent. In the constitutive equations, $Z(t,t')$ can then be replaced by the time interval $t-t'$.

As described in Sec. 2.6 above, the conventional definition of the linear viscoelastic spectra $G'(\omega), G''(\omega)$ (Eq. 11), requires not only linearity but also TTI. Thus they are well-defined only for an equilibrium state; in the SGR model, the latter exists only for $x > 1$. But even at $x > 1$ these spectra show interesting power law dependencies at low frequency; these are summarized as follows (the prefactors are omitted, but discussed by Sollich et al. (1997); Sollich (1998)):

$$\begin{array}{lllll} G'' & \propto & \omega & \text{for } 2 < x, & \propto \omega^{x-1} \quad \text{for } 1 < x < 2 \\ G' & \propto & \omega^2 & \text{for } 3 < x, & \propto \omega^{x-1} \quad \text{for } 1 < x < 3 \end{array} \tag{35}$$

Here and throughout this paper, "low frequency" in the SGR model means $\omega \ll 1$, that is, frequencies small compared to the mesoscopic attempt rate for activated hopping $\tau_0^{-1} = 1$ (in our chosen units).

Throughout its glass phase ($x \leq 1$) where the SGR model violates TTI, we must study instead the time dependent spectra $G^*(\omega, t, t_s)$ as defined in Sec. 2.6.2 above; this is done in Sec. 6.1 below. An alternative, explored by Sollich et al. (1997); Sollich (1998); Evans et al. (1999) is to observe that TTI can be restored even for $x \leq 1$ by introducing a cutoff $E_{\max}$ in the trap depth distribution $\rho(E)$. This gives interesting predictions for $x < 1$: for example, one finds $G'(\omega) \sim \omega^{1-x}$, for $\tau^{-1}(E_{\max}) \ll \omega \ll 1$ (Sollich et al., 1997; Sollich, 1998). However, this cutoff brings all ageing processes to a halt after a large finite time of order $\tau(E_{\max})$; formally there is no long term memory. Since in the present work we want to

study the ageing regime itself, we assume instead that $E_{\max}$ is infinite, so that for $x \leq 1$, ageing continues indefinitely. (This is mainly a matter of mathematical convenience. Our results would be unchanged if a largest relaxation time $\tau(E_{\max})$ was present, so long as this is much larger than all other timescales of interest.)

4.2.2 Flow Curve

The flow curve was defined in Sec. 2.7 as the nonlinear stress response $\sigma(\dot{\gamma})$ to a steady strain rate $\dot{\gamma}$. For the SGR model, it shows the following scalings:

$$\begin{array}{lcll} \sigma & \propto & \dot{\gamma} & \text{for} \quad x > 2 \\ \sigma & \propto & \dot{\gamma}^{x-1} & \text{for} \quad 1 < x < 2 \\ \sigma - \sigma_{\mathrm{y}} & \propto & \dot{\gamma}^{1-x} & \text{for} \quad x < 1 \end{array} \tag{36}$$

Here $\dot{\gamma} \ll 1$ is assumed; prefactors are discussed by Sollich (1998). The flow curve exhibits two interesting features which are explored more fully in Secs. 6.2.2 and 7.2.1. Firstly, for $x < 1$ there is a yield stress $\sigma_{\mathrm{y}}(x)$ (whose value is plotted by Sollich (1998)). A linear response regime exists at $\sigma \ll \sigma_{\mathrm{y}}$; ageing can occur for all $\sigma < \sigma_{\mathrm{y}}$. For $\sigma > \sigma_{\mathrm{y}}$ the system achieves a steady state, and ageing no longer occurs. This is because any finite flow rate, however small, causes strain-induced yielding of elements even in the deepest traps; the time required to yield, with a steady flow present, is only power law, rather than exponential in E. Thus the ageing process is curtailed or "interrupted" by flow (Sollich et al., 1997; Sollich, 1998); the flow curve is well-defined even in the glass phase. The second interesting feature is that, for $1 < x < 2$ (where ageing is absent) there is no linear response regime at all in steady shear: however small the applied stress, the behavior is dominated by strain-induced yielding. There is an anomalous (power law) relation between stress and strain rate, and an infinite zero-shear viscosity (cf. Sec. 2.7 above). This also shows up in (35), where $\eta = \lim_{\omega \to 0} G''(\omega)/\omega$ is likewise infinite.

5 Ageing in the SGR model

In this section we discuss some general features of ageing in the SGR model; in subsequent ones, we explore the rheological consequences of these phenomena.

5.1 Initial Preparation of Sample

As noted above, to solve the constitutive equations (25,26) the initial distribution $P_0(E)$ of yield energies or trap depths at time zero must be specified. Since we are interested in the rheological properties of the glass phase ($x \leq 1$), for which no steady-state distribution of yield energies exists in the absence of flow, we cannot appeal to equilibrium to fix $P_0(E)$. Instead, this should depend explicitly on the way the sample was prepared. For simplicity, we choose the case where $P_0(E) = \rho(E)$; this is equivalent to suddenly "quenching" the noise temperature x, at time zero, from a very large value ($x \gg 1$) to a value within the range of interest. We refer to it as a "deep quench".

The question of whether or not a deep quench is a good model for the sample preparation of a SGM remains open (Sollich et al., 1997; Sollich, 1998); since x is not truly a temperature, it is not clear exactly how one would realize such a quench experimentally. One argument in its favour is that this choice minimizes the information content (maximizes the entropy) of the initial distribution P_0; it is therefore a legitimate default choice when no specific information about the preparation condition is available. In any case, we expect that most interesting aspects of ageing behavior are not too sensitive to the initial quench conditions $P_0(E)$, so that a deep quench is indeed an adequate model. A study of the effect of quench depth on the results for the SGR model is summarized in App. A.4; we find independence of quench depth so long as the final noise parameter x is not too small.[3] More generally, a degree of insensitivity to the initial quench conditions is consistent with the weak long term memory scenario; a system whose response decays with a relaxation time of order its age will typically lose its memory of the initial state by a power law decay in time. This can then easily be swamped by larger, P_0-independent contributions, as indeed occurs in most regimes of the SGR model (App. A.4).

Following the initial preparation step, subsequent time evolution of the rheological response is, within the glass phase, characterized by ageing. To allow comparison with the non-ageing (but still slow) dynamics for $1 < x < 2$, below we shall also consider a similar quench from large x to values in this range.

5.2 Ageing of the Lifetime Distribution

We now (following Bouchaud (1992) and Monthus and Bouchaud (1996)) discuss in detail the way ageing affects the lifetime distribution (or equivalently the distribution of particle hopping rates) within the SGR model.

We ignore the presence of a strain; the following results apply when there is no flow, and in the linear response regime, where strain-induced hops can be ignored. Under such conditions, the hopping rate $Y(t)$ is a strain-independent function of time, and is readily found from (26) by Laplace transform. This is done in App. A.2. For the case of a deep quench (as defined above), the exact asymptotic forms of Y are as follows:

$$\begin{aligned} Y(t) &= \frac{x-1}{x} && \text{for} \quad x > 1 \\ Y(t) &= \frac{1}{\ln(t)} && \text{for} \quad x = 1 \\ Y(t) &= \frac{t^{x-1}}{x\Gamma(x)\Gamma(1-x)} && \text{for} \quad x < 1 \end{aligned} \tag{37}$$

where $\Gamma(x)$ is the usual Gamma function. These results assume $t \gg 1$, which we will usually take to be the case from now on (since timescales of experimental

[3] More precisely, if the "deep quench" specification is altered to one in which, at time zero, the system is quenched from equilibrium at $x_0 > 1$ to its final noise temperature x, the leading results are independent of x_0 so long as the final x value obeys $x > 1/(2 - 1/x_0)$. Note that this condition is never satisfied for $x < 1/2$.

interest greatly exceed the mesoscopic attempt time $\tau_0 = 1$). Note that the late-time asymptotes given here are subject to various subdominant corrections (see App. A.2), some of which are sensitive to the initial state of sample preparation. (In fact, for a quench from initial noise temperature x_0, the relative order of the affected subdominant terms becomes $t^{-x(1-1/x_0)}$. Thus, unless one quenches *from* a point that is itself only just above the glass transition, or *to* a point that has x only just above zero, the exact specification of the initial state is unimportant at late times.)

A closely related quantity to the hopping rate Y is the distribution of yield energies $P(E,t)$ – which obeys (32) – or equivalently the lifetime distribution $P(\tau,t)$. As previously pointed out, in the absence of strain, the only candidate for a steady state distribution of yield energies $P_{\rm eq}(E)$ is the Boltzmann distribution: $P_{\rm eq}(E) \propto \rho(E)\exp(E/x)$, which translates to $P_{\rm eq}(\tau) = P_{\rm eq}(E)dE/d\tau \propto \tau^{-x}$; in either language, the distribution is not normalizable for $x < 1$, leading to broken TTI in the model (Bouchaud, 1992).

Let us therefore consider a deep quench at time $t = 0$, and define the probability distribution for trap lifetimes $P(\tau, t_{\rm w})$ as a function of the time $t_{\rm w}$ elapsed since sample preparation. (In Sec. 6, we will identify $t_{\rm w}$ with the onset of a step strain.) The initial lifetime distribution, $P(\tau,0)$, describes a state in which the trap depths are chosen from the prior distribution $P(E,0) = \rho(E)$; just after a quench to temperature x the distribution of lifetimes is therefore $P(\tau,0) \propto \rho(E)d\tau/dE \propto \tau^{-(1+x)}$. Thereafter, by changing variable from E to τ in (32), we find the following approximate expressions for $P(\tau, t_{\rm w})$

$$\begin{array}{rcl} P(\tau,t_{\rm w}) & \simeq & xY(t_{\rm w})\tau\rho(\tau) \quad \text{for} \quad \tau \ll t_{\rm w} \quad \text{and} \quad t_{\rm w} \gg 1 \\ P(\tau,t_{\rm w}) & \simeq & xY(t_{\rm w})t_{\rm w}\rho(\tau) \quad \text{for} \quad \tau \gg t_{\rm w} \quad \text{and} \quad t_{\rm w} \gg 1 \end{array} \tag{38}$$

For a quench temperature above the glass point ($x > 1$), $P(\tau, t_{\rm w})$ exhibits a transient decay; as $t_{\rm w} \to \infty$, we find (using the results in (37)) that $P(\tau,t) \to P_{\rm eq}(\tau) = (1-x)\tau^{-x}$, as expected. The nature of the approach to the long time limit is illustrated schematically in Fig. 3(a); the final distribution has most of its weight at $\tau = O(1)$, consistent with the fact that the hopping rate (37) is itself $O(1)$ in this phase of the model.

For $x < 1$, in contrast, $P(\tau, t_{\rm w})$ evolves as in Fig. 3(b); the limit of $P(\tau, t_{\rm w})$ is zero for any finite τ as $t_{\rm w} \to \infty$. Hence, the proportion of elements having yield time of order unity tends to zero as $t_{\rm w} \to \infty$; the bulk of the distribution's weight is at $\tau \simeq t_{\rm w}$. (More formally, for $x < 1$, we have $\lim_{t_{\rm w}\to\infty} \int_1^b P(\tau,t_{\rm w})d\tau = 0$ for any $b > 1$, while for any $a < 1 < b$ we have instead $\lim_{t_{\rm w}\to\infty} \int_{at_{\rm w}}^{bt_{\rm w}} P(\tau,t_{\rm w})d\tau = O(1)$.) This is consistent with the decay of the hopping rate as a power law of $t_{\rm w}$, and with the idea that, in a system undergoing ageing, the characteristic relaxation time is typically of the order the age of the system itself.

5.3 Higher Moments

The above analysis focuses on the time-evolution of the distribution of elements' lifetimes, which is the usual quantity of interest in the formal analysis of ageing effects (Bouchaud and Dean, 1995; Bouchaud et al., 1998). Indeed, the latter are usually attributed to the divergence of the normalization integral, or zeroth

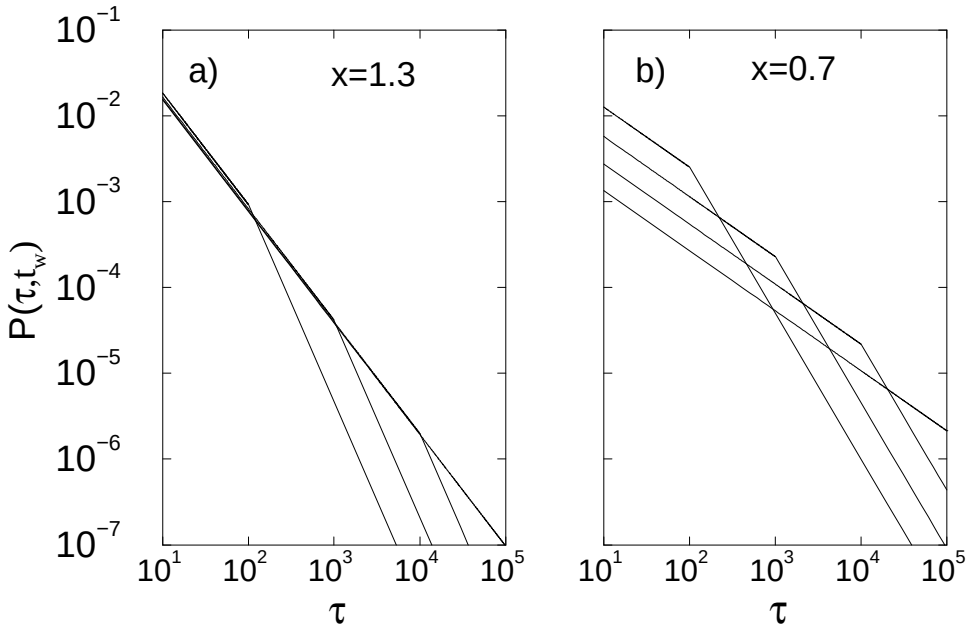

Figure 3: Schematic evolution of the relaxation time distribution (a) above the glass transition; (b) below it. The first shows a transient decay onto a steady state, the second shows ageing behavior. The curves lie in order of increasing $t_{\rm w}$ at the bottom of each figure.

moment, of $P_{\rm eq}(\tau)$ (undefined, within the Boltzmann distribution, when $x \leq 1$). Formally, however, one can consider a series of critical x values, $x_n = n+1$, below each of which the nth moment of $P_{\rm eq}$ becomes undefined (Evans et al., 1999; Odagaki, 1995). For $n > 0$ this does not lead to ageing, in the sense defined in Sec. 3 above, but can lead to anomalous, slow time evolution in any experimental measurement that probes the nth moment. For example, in Sec. 6.1.3 below, we discuss the time-evolution of the distribution of stresses borne by elements in a steady-shear startup experiment. In steady state, the stress carried by an element whose lifetime is τ is of order $\dot{\gamma}\tau$. If $P(\tau) = P_{\rm eq}(\tau)$ and is unperturbed by flow (as a linear response analysis would assume), then the zero-shear viscosity is of order $\int \tau P_{\rm eq}(\tau) d\tau$, which diverges for $x < 2$ (see Sec. 2.7 above).

6 Rheological Ageing: Imposed Strain

In this and the next sections, we describe our new rheological results for the SGR model. We focus particularly on rheological *ageing*, which occurs in the glass phase ($x < 1$); however, several new results for $1 < x < 2$, including anomalous *transient behavior*, are also presented. The case $x = 1$, which divides these regimes, shows its own especially weak (logarithmic) form of ageing and is, where necessary, treated separately below.

For simplicity, we consider (for all x values) only the idealized route to sample

preparation described in Sec. 5.1 above: the system is prepared at time $t = 0$ by means of a deep quench, so that $G_0(Z(t,0)) = G_\rho(Z(t,0))$ in the constitutive equations (25, 26). Note that these constitutive equations for the SGR model are more readily solved to find the stress response to an imposed strain, rather than vice-versa. Accordingly, we focus first on strain-controlled experiments and defer to Sec. 7 our analysis of the stress-controlled case.

6.1 Linear Response

As described in Sec. 4.2.1 above, when local strains are negligible, the SGR model displays a linear response regime. The effective time interval $Z(t,t')$ in Eqs. (25,26) becomes the actual time interval $t-t'$, and the hopping rate $Y(t')$ a strain-independent function of time. For the deep quench considered here, $Y(t')$ assumes the asymptotic forms summarized in (37). The stress response to any strain history then follows simply from (25), by integration.

6.1.1 Step Strain

For a step strain, the amplitude γ_0 gives the maximum local strain experienced by any element. The condition for linearity in this case is therefore simply $\gamma_0 \ll 1$. The linearized step strain response was defined in (3). It is found for the SGR model using (34):

$$G(t-t_{\rm w}, t_{\rm w}) = 1 - \int_{t_{\rm w}}^{t} Y(t') G_\rho(t-t')dt' \tag{39}$$

Note that by construction of the SGR model, the linear step strain response is actually identical to the correlation function defined by Bouchaud for his trap model (Bouchaud, 1992; Monthus and Bouchaud, 1996).

As outlined in App. A.3, analytic limiting forms for $G(t-t_{\rm w}, t_{\rm w})$ can be found when experimental timescales are large on the scale of the mesoscopic attempt time $\tau_0 = 1$, so that $t - t_{\rm w} \gg 1$ and $t_{\rm w} \gg 1$. In this limit we identify two distinct regimes: a short time interval regime $t - t_{\rm w} \ll t_{\rm w}$ and long time interval regime $t - t_{\rm w} \gg t_{\rm w}$ (where the measure of "short" and "long" is not now τ_0 but $t_{\rm w}$ itself). The limiting forms in each case depend on the value of x; our results are summarized in table 1.

The asymptotic scalings apparent in the various entries of table 1 can be physically motivated by the following simple arguments. Upon the application of the strain at time $t_{\rm w}$ the local strain of each element exactly follows the macroscopic one, and the instantaneous response is elastic: $G(0, t_{\rm w}) = 1$. (This is a general characteristic of the SGR model: whenever the macroscopic strain changes discontinuously by an amount $\Delta\gamma$, the stress σ also increases by $\Delta\gamma$.) In the time following $t_{\rm w}$, elements progressively yield and reset their local stresses l back to zero. The stress remaining at t will be that fraction of elements which has survived from $t_{\rm w}$ without yielding, and hence roughly that fraction $\int_{t-t_{\rm w}}^{\infty} P(\tau, t_{\rm w})\, d\tau$ which, at time $t_{\rm w}$, had time constants greater than $t - t_{\rm w}$. Hence in measuring the linear response to a step strain we are probing the properties of the system as they were at the time of strain application.

	$G(t-t_{\rm w},t_{\rm w})$ for $t-t_{\rm w}\ll t_{\rm w}$	$G(t-t_{\rm w},t_{\rm w})$ for $t-t_{\rm w}\gg t_{\rm w}$
$x>1$	$\Gamma(x)\,(t-t_{\rm w})^{1-x}$	$(x-1)\Gamma(x)\dfrac{t_{\rm w}}{(t-t_{\rm w})^{x}}$
$x=1$	$1-\dfrac{\ln(t-t_{\rm w})}{\ln(t_{\rm w})}$	$\dfrac{t_{\rm w}}{t-t_{\rm w}}\dfrac{1}{\ln(t_{\rm w})}$
$x<1$	$1-\dfrac{1}{\Gamma(2-x)\Gamma(x)}\left(\dfrac{t-t_{\rm w}}{t_{\rm w}}\right)^{1-x}$	$\dfrac{1}{\Gamma(1+x)\Gamma(1-x)}\left(\dfrac{t_{\rm w}}{t-t_{\rm w}}\right)^{x}$

Table 1: Stress response to step strain at short and long times ($t-t_{\rm w}\gg 1$, $t\gg 1$ assumed). $\Gamma(x)$ denotes the usual Gamma function.

Using the approximate expressions given in (38) above, we have $P(\tau,t_{\rm w})\propto\tau^{-x}$ for $\tau\ll t_{\rm w}$ and $P(\tau,t_{\rm w})\propto t_{\rm w}\tau^{-(1+x)}$ for $\tau\gg t_{\rm w}$. This gives, for short time intervals ($t-t_{\rm w}\ll t_{\rm w}$)

$$G(t-t_{\rm w},t_{\rm w})\simeq 1-\int_1^{t-t_{\rm w}}P(\tau,t_{\rm w})\,d\tau\simeq 1-x\,\frac{(t-t_{\rm w})^{1-x}-1}{t_{\rm w}^{1-x}-x}$$

and, for long time intervals ($t-t_{\rm w}\gg t_{\rm w}$)

$$G(t-t_{\rm w},t_{\rm w})\simeq\int_{t-t_{\rm w}}^{\infty}P(\tau,t_{\rm w})\,d\tau\simeq\frac{(1-x)t_{\rm w}(t-t_{\rm w})^{-x}}{t_{\rm w}^{1-x}-x}$$

In fact these estimates approximate the numerical data already quite well. Even better agreement is obtained by adjusting the prefactors to fit the asymptotic results in table 1:

$$G(t-t_{\rm w},t_{\rm w})\;\simeq\;1-\frac{\Gamma(x)(t-t_{\rm w})^{1-x}-1}{\Gamma^2(x)\Gamma(2-x)t_{\rm w}^{1-x}-1}\qquad\text{for } t-t_{\rm w}\ll t_{\rm w}\qquad(40)$$

$$G(t-t_{\rm w},t_{\rm w})\;\simeq\;\frac{(x-1)\Gamma(x)t_{\rm w}(t-t_{\rm w})^{-x}}{1-\Gamma(x)\Gamma(x+1)\Gamma(2-x)t_{\rm w}^{1-x}}\qquad\text{for } t-t_{\rm w}\gg t_{\rm w}\qquad(41)$$

In the relevant time regimes, these formulae agree well with our numerical results (see Fig. 4), at least over the noise temperature range 0 to 2; they could therefore be used in a standard curve fitter for comparison with experimental data. In the limit $t-t_{\rm w}\to\infty$ and $t_{\rm w}\to\infty$, they reproduce (by construction) the results shown in table 1 for $x>1$ and $x<1$. The logarithmic terms at the glass point ($x=1$) can also be recovered by taking the limit $x\to 1$ first.

Using the forms for $G(t-t_{\rm w},t_{\rm w})$ as summarized in table 1, and substituting these in Eqs. (18,19), we see that the SGR model has short term memory for

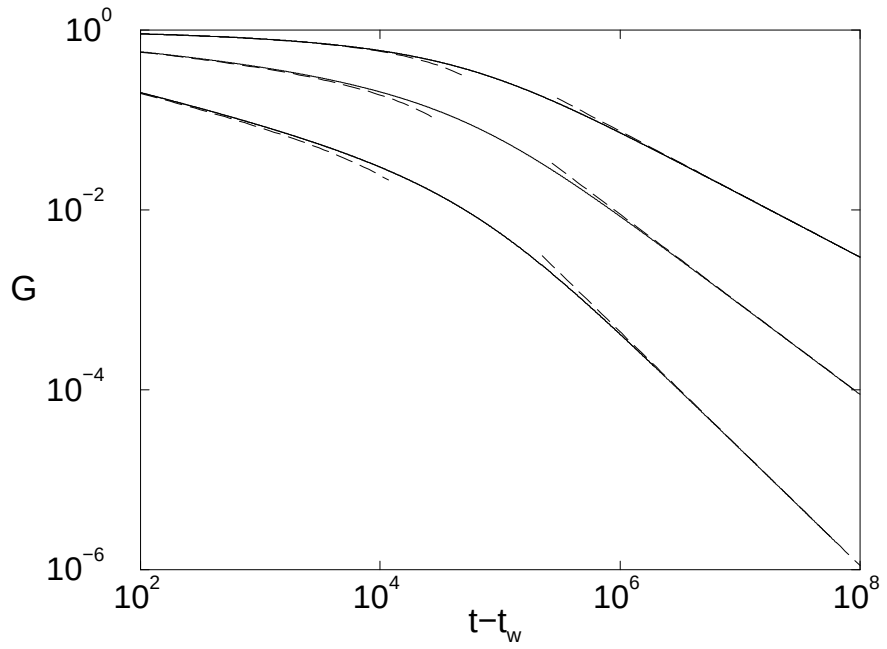

Figure 4: Approximate curves for $G(t-t_{\rm w},t_{\rm w})$ generated using the interpolating formulae (40,41) (dashed lines), compared to numerical data for this quantity (solid lines). Solid curves downwards show numerical data for G vs $t-t_{\rm w}$ at noise temperatures $x=0.7$, $x=1.0$ and $x=1.3$ respectively. The waiting time $t_{\rm w}$ is 10^5.

$x>1$ and weak long term memory for $x\leq 1$. Thus we expect transients for $x>1$ and ageing for $x\leq 1$. As shown in Fig. 5, this is indeed what we find. Transients are visible in the top left panel: the curves coincide at short time intervals $t-t_{\rm w}\ll t_{\rm w}$. At large $t_{\rm w}$, this regime accounts for more and more of the decay of G; the remaining $t_{\rm w}$-dependence is only through an unimportant tail. For $t_{\rm w}\to\infty$, the "short time" regime extends to all finite values of $t-t_{\rm w}$; one recovers the equilibrium response (shown as the dotted line) which decays to zero on a $t_{\rm w}$-independent timescale. Ageing is visible at bottom left, where the major part of the decay of G occurs on a timescale of order $t_{\rm w}$ itself, with unimportant corrections to this scaling at early times.

More generally, these step strain results for the SGR model show some interesting features of its rheology. Consider first the behavior above the glass transition ($x>1$). Here the stress decay at short time intervals ($t-t_{\rm w}\ll t_{\rm w}$) depends only upon the time interval between stress imposition and measurement itself ($t-t_{\rm w}$), and not on the sample age $t_{\rm w}$. This is because the traps which contribute to stress decay during this interval are mainly those with lifetimes $\tau<t-t_{\rm w}$; and the population of these traps has already reached Boltzmann equilibrium before the strain is switched on (see Fig. 3(a)). Taking the limit $t_{\rm w}\to\infty$ at constant $t-t_{\rm w}$, (*i.e.*, letting the system fully equilibrate *before* we apply the strain), we recover a TTI stress relaxation function which decays to

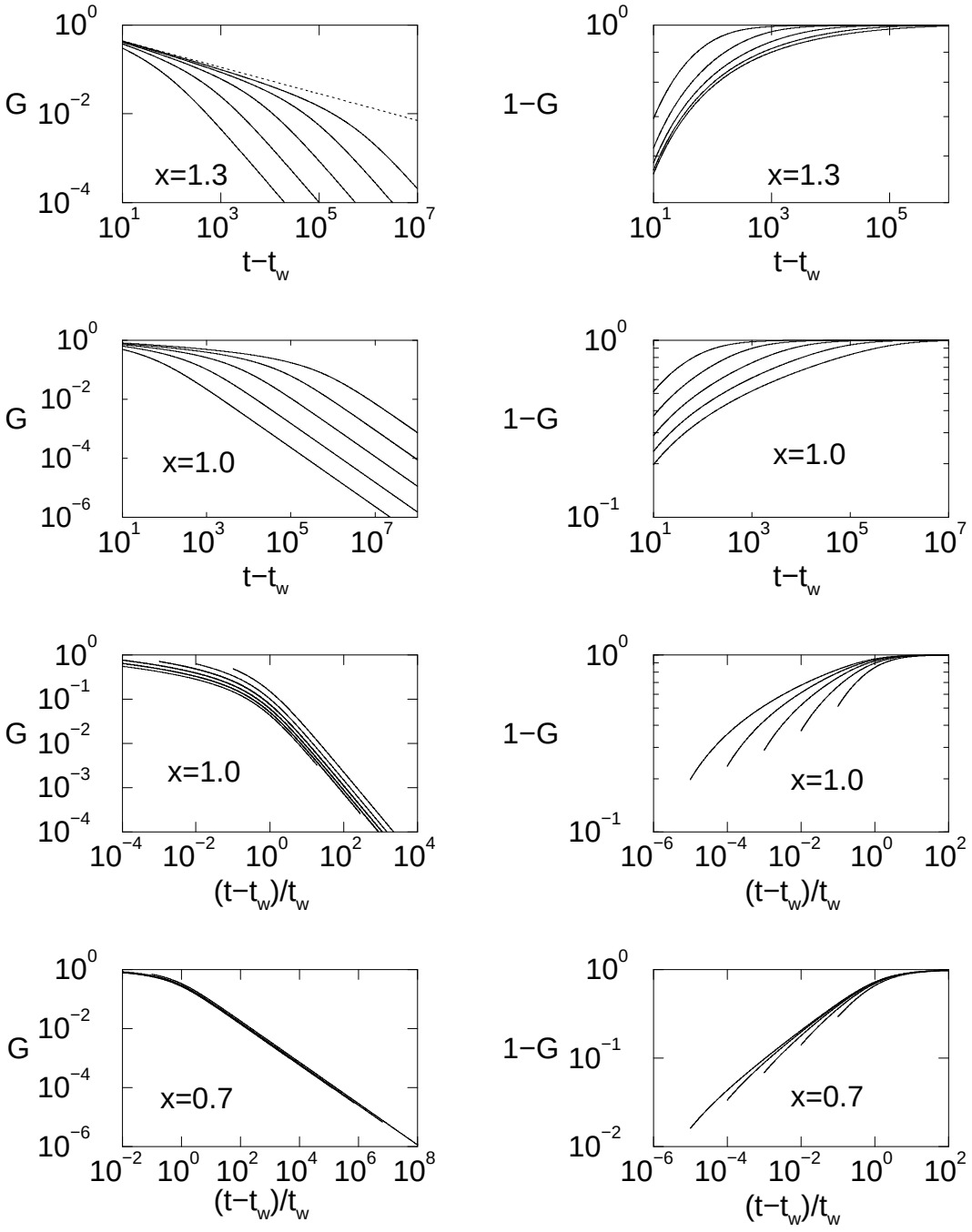

Figure 5: Left column: age-dependent stress relaxation modulus $G(t-t_{\rm w},t_{\rm w})$ against scaled time interval $(t-t_{\rm w})/t_{\rm w}$ (for $x \leq 1$) and time interval $t-t_{\rm w}$ (for $x \geq 1$). Right column: $1-G(t-t_{\rm w},t_{\rm w})$, plotted similarly. Shown are data for waiting times $t_{\rm w} = 10^2\,, 10^3 \ldots 10^6$ (left to right for top four graphs, right to left for bottom four graphs).

zero on timescales of order $\tau_0 = 1$. On the other hand, for any finite waiting time t_w, the stress decay at long enough times ($t - t_w \gg t_w$) violates TTI, since it is controlled by decay out of deep traps ($\tau \gg t_w$) which had not already equilibrated before t_w. Note that even though this feature of the stress relaxation depends explicitly on t_w, it is not an ageing effect according to our definition in Sec. 3. This is because the deviations from TTI and the dependence on t_w manifest themselves at ever smaller values of G as t_w becomes large. Equivalently, if we assume that $G(t - t_w, t_w)$ can be measured reliably only as long as it remains greater than some specified value (a small fraction ϵ of its initial value $G(0, t_w) = 1$, for example), then the results will become t_w-independent for sufficiently large t_w.

Below the glass point ($x \leq 1$) we see true ageing, rather than anomalous transient effects: A significant part of the stress relaxation $G(t - t_w, t_w)$ now takes place on timescales that increase with the sample age t_w itself. In fact, in the case of the SGR model, this applies to the *complete* stress relaxation, and t_w itself sets the relevant timescale: for $x < 1$, G depends on time only through the ratio $(t - t_w)/t_w$. It is still true that stress decay during the interval $t - t_w$ is dominated by traps for which $\tau < t - t_w$, but no longer true that these traps have reached Boltzmann equilibrium by time t_w: in an ageing system such equilibrium is never attained, even for a subset of shallow traps (see Fig. 3(b)). Instead, the population of such traps will gradually deplete with age, as the system explores ever-deeper features in the energy landscape. Decay from these deep traps becomes ever slower; the limit $t_w \to \infty$ (for any finite $t - t_w$) gives completely arrested behavior in which all dynamics has ceased, and the system approaches a state of perfect elasticity ($G = 1$). Even in an experiment that can only resolve values of G above a threshold ϵ (see above), we would detect that the stress relaxation becomes slower and slower as t_w increases.

The fact that G depends on time only through the ratio $(t - t_w)/t_w$ is typical, but not automatic for ageing systems; the case $x = 1$, for example, does not have it. It is a simple example of Struik's 'time ageing-time superposition' principle (Struik, 1978): the relaxation curves for different t_w can be superposed by a rescaling of the time interval $t - t_w$ by the sample age. However, as mentioned previously, Struik's discussion allows a more general form in which the scale factor varies as t_w^μ, with $\mu \leq 1$. Even more generally, the timescale for ageing can be any monotonically increasing and unbounded function of t_w. There can also be *parts* of the stress relaxation which still obey TTI. (An example is $G(t - t_w, t_w) = g_1(t - t_w) + g_2((t - t_w)/t_w)$, which exhibits ageing when g_2 is nonzero, but also has a TTI short time part described by g_1.) Superpositions of relaxations with different ageing timescales are also possible; compare Eq. (20). The SGR model exemplifies the simplest type of ageing behavior only.

6.1.2 Oscillatory Strain

In an oscillatory strain, the maximal local strain of any element is γ_0, the strain amplitude. Thus a linear regime in the SGR model is ensured whenever $\gamma_0 \ll 1$. The linear viscoelastic spectrum, as defined in (10), can be found for the SGR

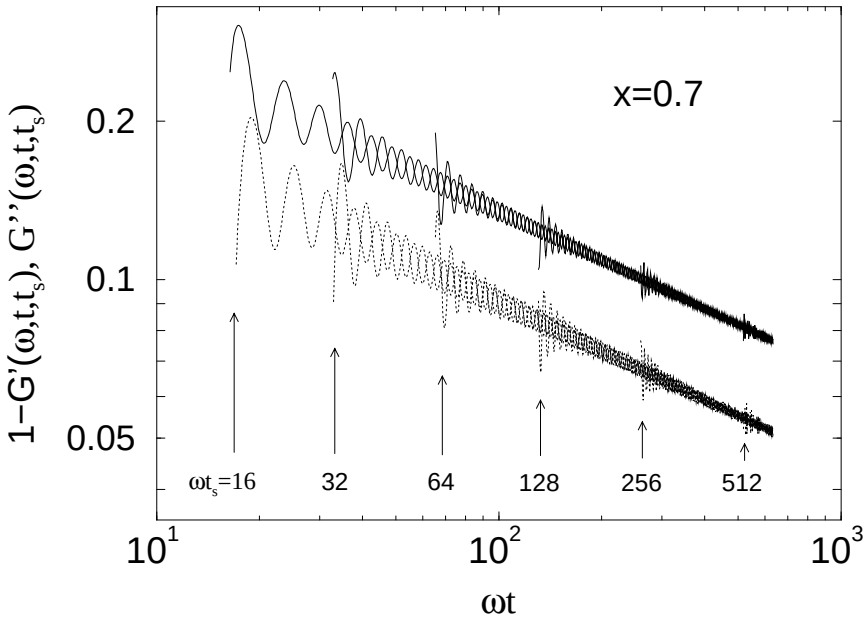

Figure 6: Demonstration of $t_{\rm s}$-independence $G^*(\omega,t,t_{\rm s})$ in the glass phase. Shown are $1-G'(\omega,t,t_{\rm s})$ (solid lines) and $G''(\omega,t,t_{\rm s})$ (dotted lines) against ωt. The noise temperature is $x=0.7$ and the frequency $\omega=0.01$. Start-time values $t_{\rm s}$ obey $\omega t_{\rm s}=2^4\,,2^5\,,\ldots 2^9$. When $\omega(t-t_{\rm s})\gg 1$ (a sufficient number of oscillations after the beginning of each dataset) and $\omega t_{\rm s}\gg 1$ (datasets beginning further on the right), G^* becomes independent of $t_{\rm s}$.

model using (34):

$$G^*(\omega,t,t_{\rm s})=1-\int_{t_{\rm s}}^{t}e^{-i\omega(t-t')}Y(t')G_\rho(t-t')dt' \tag{42}$$

In principle, this quantity depends on $t_{\rm s}$, the time when the oscillatory strain was started. However, when the experimental timescales become large, we find (as shown in App. B) that this dependence on $t_{\rm s}$ is weak. In fact, within the SGR model, the conditions needed to make G^* negligibly dependent on $t_{\rm s}$ (for low frequencies, $\omega\ll 1$) are that $\omega(t-t_{\rm s})\gg 1$ and $\omega t_{\rm s}\gg 1$. The first signifies merely that many cycles of oscillatory strain are performed before the stress is measured; the second ensures that transient contributions from the initial sample preparation stage (the quench at $t=0$) are negligible. Notably, these criteria do not depend on the noise temperature x, and therefore hold even in the glass phase ($x\leq 1$); see Fig. 6. The fact that they are sufficient even in the glass phase is far from obvious physically, and requires a careful discussion: we give this in App. B. Broadly speaking, these criteria are satisfied in any experiment that would reliably measure a conventional $G^*(\omega)$ spectrum for systems with TTI.

For the purposes of such experiments, we can therefore drop the $t_{\rm s}$ argument and define a time-dependent spectrum $G^*(\omega,t)$. Our results for the long-time

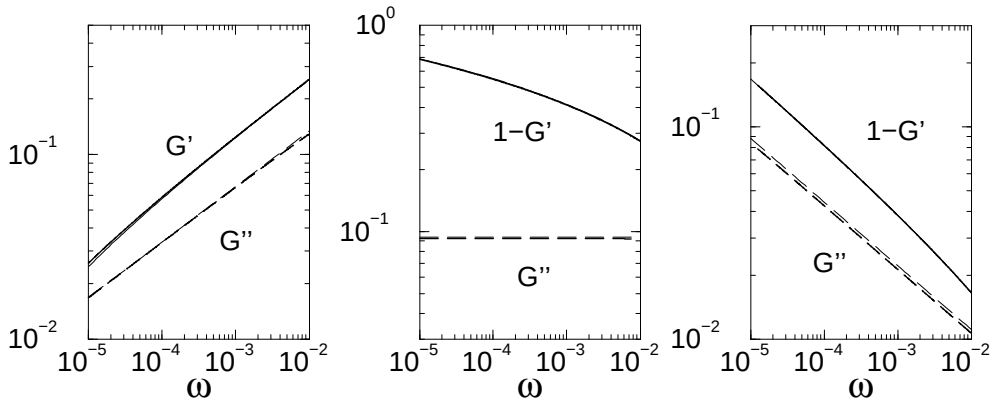

Figure 7: Approximate curves for $G'(\omega,t)$ and $G''(\omega,t)$ generated using the simple interpolating formula (44) (thin lines) compared to the numerical data for these quantities (thick lines), plotted as a function of ω at fixed $t = 10^7$, and $x = 1.3, 1, 0.7$. Note that the predictions of the interpolating formula are practically indistinguishable from the numerical data over the frequency window shown.

behavior ($t \gg 1$) of this quantity are as follows (see App. A.3):

$$\begin{aligned} G^*(\omega,t) &= \Gamma(x)\Gamma(2-x)(i\omega)^{x-1} \quad \text{for} \quad 1<x<2 \\ G^*(\omega,t) &= 1+\frac{\ln(i\omega)}{\ln(t)} \qquad\qquad\quad \text{for} \quad x=1 \\ G^*(\omega,t) &= 1-\frac{1}{\Gamma(x)}(i\omega t)^{x-1} \qquad\quad \text{for} \quad x<1 \end{aligned} \tag{43}$$

For comparison with experimental results, the simple interpolating form

$$G^*(\omega,t) = 1 - \frac{\Gamma(x)\Gamma(2-x)\,(i\omega)^{x-1}-1}{\Gamma^2(x)\Gamma(2-x)t^{1-x}-1} \tag{44}$$

may be useful; we have checked that it provides a good fit to our numerical data, at least over the noise temperature range 0.7 to approximately 1.3 (see Fig. 7).

By measuring $G^*(\omega,t)$ we are directly probing the properties of the system at the time of measurement, t. In light of this, the results of (43) are easily understood. In the ergodic phase ($x > 1$), $G^*(\omega,t)$ will reach a t-independent value within a time of $O(1/\omega)$ after the quench, as the relevant traps will then have attained their equilibrium population. The relaxation time is then of $O(\tau_0)$ (that is, $O(1)$ in our units) and the response $G^*(\omega,t)$ is a function only of ω. In contrast, below the glass point the characteristic relaxation time at the epoch of measurement is of order t, and the response is a function only of the product ωt. Since the losses in an oscillatory measurement arise from traps with lifetimes less than about $1/\omega$ (elements in deeper traps respond elastically), the overall response becomes more elastic as the system ages into traps with $\tau > 1/\omega$.

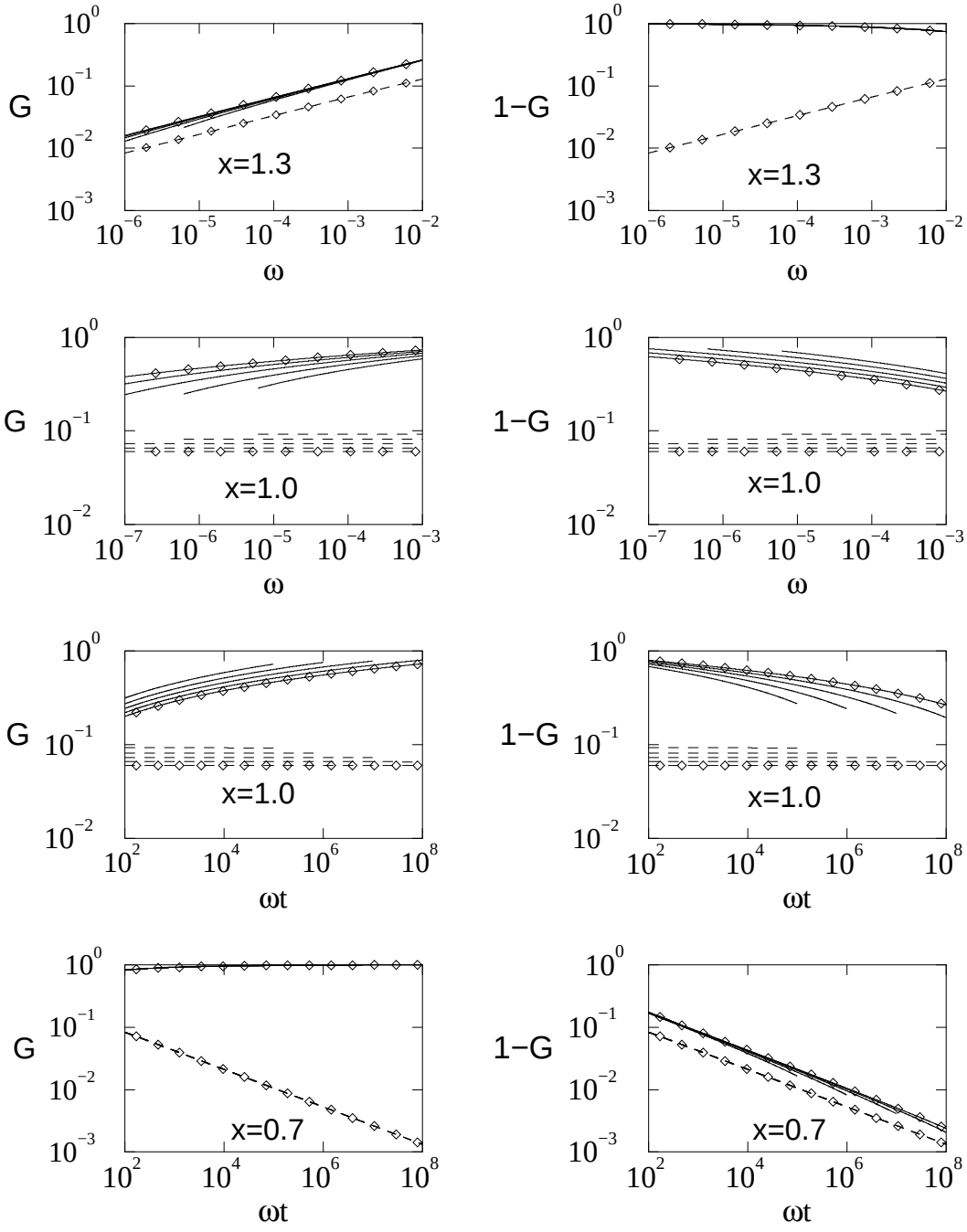

Figure 8: Left column: viscoelastic spectra $G'(\omega)$ (solid lines) and $G''(\omega)$ (dashed lines) versus frequency, ω (for $x \geq 1$) or scaled frequency ωt (for $x \leq 1$). Right column: frequency-dependent corrections to Hookean elasticity, $1 - G'$ (solid lines), G'' (dashed lines). Data are shown for systems aged $t = 10^7, 10^8, \ldots 10^{11}$. At any fixed ω the curves lie in order of age; data on the oldest system is marked by the symbols.

Numerical results for the viscoelastic spectrum $G^*(\omega, t)$ at various measurement times t for various x are shown in Fig.8. These indeed show a characteristic "hardening" of the glassy material as it ages: the storage modulus at low frequencies evolves upwards, and the loss modulus downward (Sollich et al., 1997; Sollich, 1998). There is good data collapse both above and below the glass point (with the appropriate scalings); the data for $x = 1$ do not collapse in either representation due to logarithmic terms. If plotted against ω rather than ωt, the data for $x = 0.7$ would resemble Fig. 1. Each spectrum terminates at frequencies of order $\omega t \simeq 1$. This is because one cannot measure a true oscillatory response for periods *beyond* the age of the system. Therefore, the rise at low frequencies in G' spectra like Fig. 1 represents the ultimate rheological behavior. (Note that this only applies for $\mu = 1$ in Struik's scheme, as exemplified by the SGR model. Whenever $\mu < 1$, the region to the left of the loss peak can, in principle, be accessed eventually.)

It is shown in App. B that the insensitivity of $G^*(\omega, t, t_s)$ to t_s in practical measurements of the viscoelastic spectrum (where an oscillatory strain is maintained over many cycles) arises because (even when $x < 1$) the most recently executed strain cycles dominate the stress response at time t. In essence, as long as an oscillatory strain was started many cycles ago, there is no memory of when it was switched on; accordingly (by linearity) an oscillatory strain started in the distant past and then switched off at t_s, will leave a stress that decays on a timescale comparable to the period of the oscillation. This is markedly different from non-oscillatory stresses, where long term memory implies that the response to a step strain, applied for a long time, persists for a similarly long time after it is removed (see Sec. 3 above). Thus the fact that the SGR glass "forgets" the t_s argument of $G^*(\omega, t, t_s)$, is directly linked to the oscillatory nature of the perturbation. As also shown in App. B, this forgetfulness means that, in the SGR model, a Fourier relationship between oscillatory and step strain responses is recovered; to a good approximation, one has the relation (13)

$$G^*(\omega, t) = i\omega \int_0^\infty e^{-i\omega t'} G(t', t)\, dt' \tag{45}$$

Apart from the explicit dependence on the measurement time[4] t, this is the usual (TTI) result. But here it is nontrivial because of ageing effects. As discussed at the end of Sec. 3, we speculate that the relation (45) holds not only for the SGR model, but in fact for all systems which have only *weak* long term memory. We also note that (45) can formally be used to *define* $G^*(\omega, t)$ in the range of small frequencies $\omega < 1/t$, where it would reflect the behavior of the step response $G(t', t)$ in for long times $t' \gg t$. But in this frequency regime $G^*(\omega, t)$ can no longer be related to a physical measurement of the stress response to an oscillatory strain; as pointed out above, such a measurement always requires at least one period of oscillation and thus $\omega t > 1$.

[4]Formally, t appears as the time at which an step strain was initiated, or an oscillatory measurement ended. Thus $G^*(\omega, t)$ is to within $i\omega$, the Fourier transform of the step strain response function $G(\Delta t, t)$ that would be measured if a step strain were applied immediately *after* the oscillatory measurement had been done.

6.1.3 Startup of Steady Shear

Consider now a startup experiment in which a steady shear of rate $\dot{\gamma} \ll 1$ begins at time $t_{\rm w}$. So long as we restrict attention to times short enough that the total strain remains small ($\dot{\gamma}(t - t_{\rm w}) \ll 1$) the system remains in a linear response regime. (This contrasts with the ultimate steady-state behavior which, for $x < 2$, is always nonlinear; the crossover to a nonlinear regime at late times is discussed in Sec. 6.2.2 below.)

Within the regime of linear response, any element's lifetime is independent of strain and obeys $\tau = \exp(E/x)$. As described in Sec. 5.2 above, at a time t after a deep quench, the distribution of lifetimes obeys $P(\tau, t) \sim \tau\rho(\tau)$ for $\tau \ll t$ and $P(\tau, t) \sim t\rho(\tau)$ for $\tau \gg t$. Since the local stress associated with a given trap is of order $\dot{\gamma}\tau$ for $\tau \ll t - t_{\rm w}$, and $\dot{\gamma}(t - t_{\rm w})$ for $\tau \gg t - t_{\rm w}$, we can construct an estimate of the macroscopic stress; for $t - t_{\rm w} \ll t_{\rm w}$,

$$\begin{aligned} \sigma(t) &\simeq \frac{\dot{\gamma}\left[\int_1^{t-t_{\rm w}} \tau^2\rho(\tau)d\tau + (t-t_{\rm w})\int_{t-t_{\rm w}}^{t} \tau\rho(\tau)d\tau + (t-t_{\rm w})t\int_t^\infty \rho(\tau)d\tau\right]}{\int_1^t \tau\rho(\tau)d\tau + t\int_t^\infty \rho(\tau)d\tau} \\ &\simeq \frac{\dot{\gamma}\left[x(t-t_{\rm w})^{2-x} + (x-2)(t-t_{\rm w})t^{1-x} + x(1-x)\right]}{(x-2)\left(t^{1-x} - x\right)} \end{aligned} \tag{46}$$

This gives, for long times and in the linear response regime, $\sigma(t) \sim \dot{\gamma}(t - t_{\rm w})$ for $x < 1$ (which is purely elastic behavior), $\sigma(t) \sim \dot{\gamma}(t - t_{\rm w})^{2-x}$ for $1 < x < 2$ (which is an anomalous power law), and $\sigma(x) \sim \dot{\gamma}$ for $x > 2$; repeating the same calculation with $t \gg t_{\rm w}$ gives the same asymptotic scaling in each case. An asymptotic analysis of the constitutive equations confirms these scalings, with prefactors as summarized in table 2. Because the results depend only on $t - t_{\rm w}$, any explicit dependence on $t_{\rm w}$ must reside in subdominant corrections to these leading asymptotes. Accordingly, *linear* shear startup is not a good experimental test of ageing or slow transient effects. The power law anomaly for $1 < x < 2$ can be understood by examining which traps make dominant contributions to $\sigma(t) = \int s(\tau, t)d\tau$. (Recall that $s(\tau, t)d\tau$ is the stress contribution at time t from elements of lifetime τ; see Sec. 4.1.) For $x > 2$, $s(\tau, t)$ is weighted strongly toward traps of lifetime $O(1)$; hence $\sigma(t)$ tends to a finite limit (of order $\dot{\gamma}$) as $t \to \infty$, and the viscosity of the system is finite. For $x < 2$, on the other hand, most of the weight in the $s(\tau, t)$ distribution involves lifetimes of order t. As time passes, stress is carried by deeper and deeper traps, and (in the absence of flow-induced yielding) the mean stress diverges as $t \to \infty$.

In fact, as discussed in Sec. 5.3 above, just as the Boltzmann distribution for the relaxation times $P_{\rm eq}(\tau) = P(\tau, \infty) \sim \tau\rho(\tau)$ is non-normalisable for $x \leq 1$ (giving glassiness and ageing), so, in the absence of strain-induced yielding, is the ultimate distribution $s(\tau, \infty) \sim \tau^2\rho(\tau)$ of stresses residing in traps of lifetime τ, whenever $x < 2$. The zero shear viscosity η is therefore infinite throughout this regime, as noted previously.

6.2 Nonlinear Response

We now turn to the nonlinear behavior of the SGR model under imposed strain, starting with the step strain case.

	$\frac{\sigma(t-t_{\rm w},t_{\rm w})}{\dot\gamma}$ for $t-t_{\rm w}\ll t_{\rm w}$	$\frac{\sigma(t-t_{\rm w},t_{\rm w})}{\dot\gamma}$ for $t-t_{\rm w}\gg t_{\rm w}$
$2<x$	$\frac{x-1}{x-2}$	$\frac{x-1}{x-2}$
$1<x<2$	$\frac{\Gamma(x)}{2-x}(t-t_{\rm w})^{2-x}$	$\frac{(x-1)\Gamma(x)}{2-x}(t-t_{\rm w})^{2-x}$
$x<1$	$(t-t_{\rm w})$	$(1-x)(t-t_{\rm w})$

Table 2: Stress response to shear strain of constant rate $\dot\gamma$ at short and long times ($t-t_{\rm w}\gg 1$, $t\gg 1$, $\dot\gamma\ll 1$ assumed). These results apply to the regime $\dot\gamma(t-t_{\rm w})\ll 1$, where strain-induced yielding can be neglected, making the response linear.

6.2.1 Step Strain

The nonlinear step strain response function was defined in (3). It is found for the SGR model from (34):

$$G(t-t_{\rm w},t_{\rm w};\gamma_0)=G_0(Z(t,0))+\int_0^{t_{\rm w}}Y(t')G_\rho(Z(t,t'))dt' \tag{47}$$

where, using (27):

$$Z(t,t')=(t-t_{\rm w})\exp\left(\gamma_0^2/2x\right)+(t_{\rm w}-t') \tag{48}$$

On the other hand, in the linear regime we have:

$$\begin{aligned} G(t-t_{\rm w},t_{\rm w},\gamma_0\to 0) &\equiv G(t-t_{\rm w},t_{\rm w}) \\ &= G_0[(t-t_{\rm w})+(t_{\rm w}-0)] \\ &\quad +\int_0^{t_{\rm w}}Y(t')G_\rho\left[(t-t_{\rm w})+(t_{\rm w}-t')\right]dt' \end{aligned} \tag{49}$$

Direct comparison of (47) and (49) reveals that:

$$G(t-t_{\rm w},t_{\rm w};\gamma_0)=G\left((t-t_{\rm w})\exp\left(\gamma_0^2/2x\right),t_{\rm w}\right) \tag{50}$$

This result generalizes that of Sollich (1998) for the non-ageing case ($x>1$). It can be understood as follows. Within the SGR model, instantaneous response to a step strain at $t_{\rm w}$ is always elastic (that is, $G(0,t_{\rm w},\gamma_0)=1$); the fraction of stress remaining at time $t>t_{\rm w}$ is the fraction of elements which have survived from $t_{\rm w}$ to t without yielding (see Sec. 6.1.1 above). The stress decay is therefore

determined entirely by the distribution of relaxation times in the system just after the strain is applied at time t_w. The effect of a finite strain is solely to modify the distribution of barrier heights, and hence to modify this distribution of relaxation times τ; in fact (within the model) nonlinear strain reduces the yield time of every element by an identical factor of $\exp(\gamma_0^2/2x)$ (Sollich, 1998). Thus the relaxation after a nonlinear step strain at t_w is found from the linear case by rescaling the time interval $t - t_w$ using this same factor. Accordingly, the asymptotic results given for $G(t - t_w, t_w)$ in table 1 can be converted to those for the nonlinear regime by replacing the time interval $t - t_w$ by a strain-enhanced value $(t - t_w)\exp(\gamma_0^2/2x)$, wherever it appears there.

6.2.2 Startup of Steady Shear

In Sec. 6.1.3 we discussed the response to start up of steady shear (with $\dot{\gamma} \ll 1$) at time t_w; we assumed there that a linear response was maintained. Let us now consider the effect of strain-induced yield events, which cause nonlinearity. Consider first what happens for $x > 2$ (where the SGR model predicts Newtonian fluid behavior for $\dot{\gamma} \ll 1$). Here the main stress contribution is from elements which, were they unstrained, would have lifetime $\tau(E) = \exp(E/x)$ of order unity. So, if the strain rate obeys $\dot{\gamma} \ll 1$, these elements will acquire only negligible stress before they yield spontaneously. Hence their lifetimes are not affected by strain, and the stress response remains linear at all times, including the steady state limit: $\sigma(t \to \infty) \to \eta\dot{\gamma}$.

We therefore focus on the case $x < 2$, where nonlinearities do appear. The dominant stress contributions in this regime are from deep traps, *i.e.*, elements with lifetimes of order t. Linearity applies only if such elements are unlikely to undergo strain-induced yielding before they yield spontaneously, after a time of order t. Such elements carry strains of order $\dot{\gamma}t$, which enhances their yield rate by a factor $\exp[(\dot{\gamma}t)^2/2x]$; we require that this is small, which holds only so long as $\dot{\gamma}t \ll 1$. Hence the predictions of the linear theory of Sec. 6.1.3 can be maintained to arbitrarily long times only by taking the limit $\dot{\gamma} \to 0$ before one takes the steady state limit of $t \to \infty$. This means that the width of the linear response regime in steady flow is vanishingly small for $x < 2$, as previously discussed.

As mentioned in Sec. 6.1.3, throughout the linear period the startup curve shows no strong ageing or transient effects, even though the stress is evolving into deeper traps. At finite $\dot{\gamma}$, the linear period ends at $t \simeq \dot{\gamma}^{-1}$ (within logarithmic terms, discussed below); at later times, the main stress-bearing elements will, during their lifetimes, become strongly strained. Indeed, at strain rate $\dot{\gamma}$, an element with yield energy E will be strained to the top of its yield barrier in a time $t_{\rm int} \simeq E^{1/2}/\dot{\gamma} \simeq (\log\tau)^{1/2}/\dot{\gamma}$. The tendency of the stress distribution $s(\tau, t)$ (and also, for any $x < 1$, the lifetime distribution $P(\tau, t)$) to evolve toward deeper and deeper traps is thereby *interrupted*: the lifetime of a deep trap is converted from τ to a much smaller value, of order $(\log\tau)^{1/2}/\dot{\gamma}$ (Sollich et al., 1997; Sollich, 1998). This truncation of the lifetime distribution is enough to ensure that these distributions are never dominated by the deep traps, and a steady state is recovered; accordingly, there are no ageing effects at late enough

times either.

Note, however, that the stress at the end of the linear regime can be higher than the steady state value, leading to an overshoot in the startup curve; see Sollich (1998). This overshoot region, unlike the two asymptotes, shows a significant dependence on the system age $t_{\rm w}$, as shown in Fig. 9. The physics of this is clear: the extent of the linear regime gets progressively larger as $t_{\rm w}$ is increased, because the system has aged into deeper traps (and because the SGR model assumes that within each trap the relation between stress and strain is linear). Thus the strain at which strong yielding sets in increases (roughly logarithmically) with $t_{\rm w}$; the height of the overshoot is accordingly increased before dropping onto the same, $t_{\rm w}$-independent, steady-shear plateau.

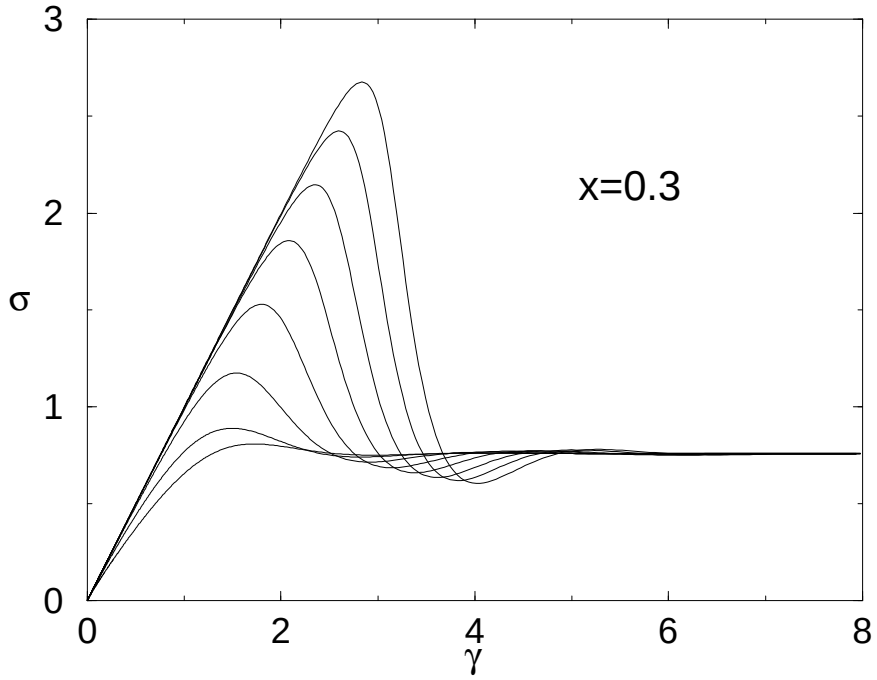

Figure 9: Stress response σ, in shear startup, vs strain γ at noise temperature $x = 0.3$ and strain rate $\dot{\gamma} = 0.001$. Curves from bottom to top correspond to increasing ages $t_{\rm w} = 10^2\,, 10^3 \ldots 10^9$ at time of startup.

7 Rheological Ageing: Imposed Stress

We now analyse the SGR model's predictions for various stress-controlled rheological experiments. (We continue to assume the sample to have been prepared at time $t = 0$ by the idealized "deep quench" procedure defined in Sec. 5.1.) As previously remarked, the structure of the constitutive equations makes the analysis more difficult for imposed stress than for imposed strain. The following discussion is therefore largely based on our numerical results, with asymptotic analysis of a few limiting cases. Our numerical method is outlined in App. C.2.

7.1 Linear Response

7.1.1 Step Stress

The SGR model predicts that upon the application of a step stress there will be an instantaneously elastic response. Elements then progressively yield and reset their local stresses to zero; thus we must apply progressively more strain to maintain the macroscopic stress at a constant value. Strain thus increases with time, but at a rate that could tend to zero at long times. Potentially therefore, individual elements can acquire large local strains and, just as in the shear startup case, linearity of the response need not be maintained at late times. As we did for shear startup, we therefore first proceed by assuming that the response *is* linear; we find the corresponding $\gamma(t)$ and then (in Sec. 7.2 below) consider *a posteriori* up to what time t the linear results remain valid.

In the linear regime the step stress response is described by the creep compliance $J(t-t_{\rm w},t_{\rm w})$ which was defined in Sec. 2.5. We computed this quantity numerically from the linearized form of the constitutive equation (34) for the SGR model, which for step stress may be written

$$1 = J(t-t_{\rm w},t_{\rm w}) - \int_{t_{\rm w}}^{t} J(t'-t_{\rm w},t_{\rm w})Y(t')G_\rho(t-t')dt' \qquad (51)$$

In analysing our numerical results we first identify, as usual, regimes of short and long time interval between stress onset and measurement, $t-t_{\rm w} \ll t_{\rm w}$ and $t-t_{\rm w} \gg t_{\rm w}$ respectively. (We assume again that $t-t_{\rm w} \gg 1$ and $t_{\rm w} \gg 1$.) In these two regimes we find the time dependences summarized in table 3. For the long time interval regime ($t-t_{\rm w} \gg t_{\rm w}$), the results were in fact obtained as follows. Curves for $J(t-t_{\rm w},t_{\rm w})$ were first generated numerically; the observed scalings (for example, $J \sim (t-t_{\rm w})^{x-1}$ for $1<x<2$) were then taken as ansätze for analytic substitution into the constitutive equation (51). In each case this allowed us to confirm the given functional form, and to compute exactly the x-dependent prefactors shown. These prefactors were cross-checked by comparison with the numerical results; no discrepancies were found.

To obtain results for short time intervals, we proceeded by assuming that the resulting compliance $J(t-t_{\rm w},t_{\rm w})$ is the same as if we first let $t_{\rm w}\to\infty$ (the dominant traps are in Boltzmann equilibrium; see Fig. 3a); this limits the analysis to $x>1$. (For $x<1$, we find instead $J = 1+{\rm const}\times[(t-t_{\rm w})/t_{\rm w}]^{1-x}$ at very early times; but this breaks down as soon as the second term becomes comparable to the leading, elastic, result.) The resulting prediction of $J(t-t_{\rm w},t_{\rm w}\to\infty)$ was found analytically from $G(t-t_{\rm w},t_{\rm w}\to\infty)$ and the reciprocal relations between the corresponding Fourier transforms (see Sec. 2.6 above); these were again checked numerically.

Further insight into the results of table 3 can be gained as follows. In step stress, we need to keep applying larger and larger strains because elements progressively yield and reset their local stresses to zero. To maintain constant stress, the rate at which stress increases due to straining (which in our units is just the strain rate $\dot\gamma$) must match the rate at which stress is lost, due to local yielding events. The latter defines a "stress-weighted hopping rate" $Y_s = \int \tau^{-1}s(\tau,t)d\tau$. For $x>2$, Y_s remains a constant of order σ_0; stress remains in traps of lifetime

	$J(t-t_{\rm w},t_{\rm w})$ for $t-t_{\rm w}\ll t_{\rm w}$	$J(t-t_{\rm w},t_{\rm w})$ for $t-t_{\rm w}\gg t_{\rm w}$
$x>2$	$\dfrac{x-2}{x-1}\,(t-t_{\rm w})$	$\dfrac{x-2}{x-1}\,(t-t_{\rm w})$
$1<x<2$	$\dfrac{(t-t_{\rm w})^{x-1}}{\Gamma^2(x)\Gamma(2-x)}$	$\dfrac{(t-t_{\rm w})^{x-1}}{\Gamma^2(x)\Gamma(2-x)-\Gamma(x)}$
$x=1$	—	$\dfrac{3}{\pi^2}\ln^2(t-t_{\rm w})$
$x<1$	—	$\dfrac{1}{\psi(1)-\psi(x)}\ln\left(\dfrac{t-t_{\rm w}}{t_{\rm w}}\right)$

Table 3: Linear creep compliance in the SGR model at long and short times ($t-t_{\rm w}\gg 1$, $t_{\rm w}\gg 1$ assumed). $\Gamma(x)$ denotes the Gamma function, and $\psi(x)=\Gamma'(x)/\Gamma(x)$. The blank entries for $x<1$ are explained in the text.

$\tau=O(1)$ and the creep response is purely viscous. For $x<2$, however, Y_s decays as a power law of $(t-t_{\rm w})$; the stress distribution $s(\tau,t)$ is dominated at time t by traps with lifetimes τ of order $t-t_{\rm w}$, the time interval since the stress application. (In fact, $Y_s\sim\dot\gamma\sim(t-t_{\rm w})^y$ where $y=x-2$ for $1<x<2$ and $y=-1$ for $x<1$.)

For $1<x<2$, the scenario given above for the time-dependence of Y_s is closely analogous to that given in Sec. 5.2 above for the hopping rate $Y=\int\tau^{-1}P(\tau,t)d\tau$ in systems with $x<1$. Indeed, the evolution of Y_s following a step stress, at noise temperature x, is closely related[5] to that of Y, following a quench, at noise temperature $x-1$.

The ageing behavior of the linear creep compliance $J(t-t_{\rm w},t_{\rm w})$ shows significant differences from the step strain modulus $G(t-t_{\rm w},t_{\rm w})$ discussed in Sec. 6.1.1 above. In the glass phase ($x<1$), the strain response to step stress indeed depends on age: it is a function of $(t-t_{\rm w})/t_{\rm w}$ as expected (see Fig. 10). However, the dependence (for long time intervals) is only logarithmic; $J(t-t_{\rm w},t_{\rm w})\sim\ln\left((t-t_{\rm w})/t_{\rm w}\right)=\ln(t-t_{\rm w})-\ln t_{\rm w}$ (see table 3) which means that in the long time interval limit ($t-t_{\rm w}\gg t_{\rm w}$) the explicit waiting time dependence ($\ln t_{\rm w}$) represents

[5]More generally one can show for the SGR model that, for an *equilibrium* system whose noise temperature is $x>1$, the evolution of the stress distribution $s(\tau,t)$ following application of a step stress at $t=0$ is, at long times, equivalent to that of the probability distribution $P(\tau,t)$, in a system deep-quenched to a noise temperature $x-1$ at $t=0$. This result is connected with the discussion made in Sec. 5.3 above, of the variation with x of the dynamics of successive moments of the lifetime distribution: at noise temperature $x+n$, the dynamics of the nth moment is like that of the zeroth moment at noise temperature x.

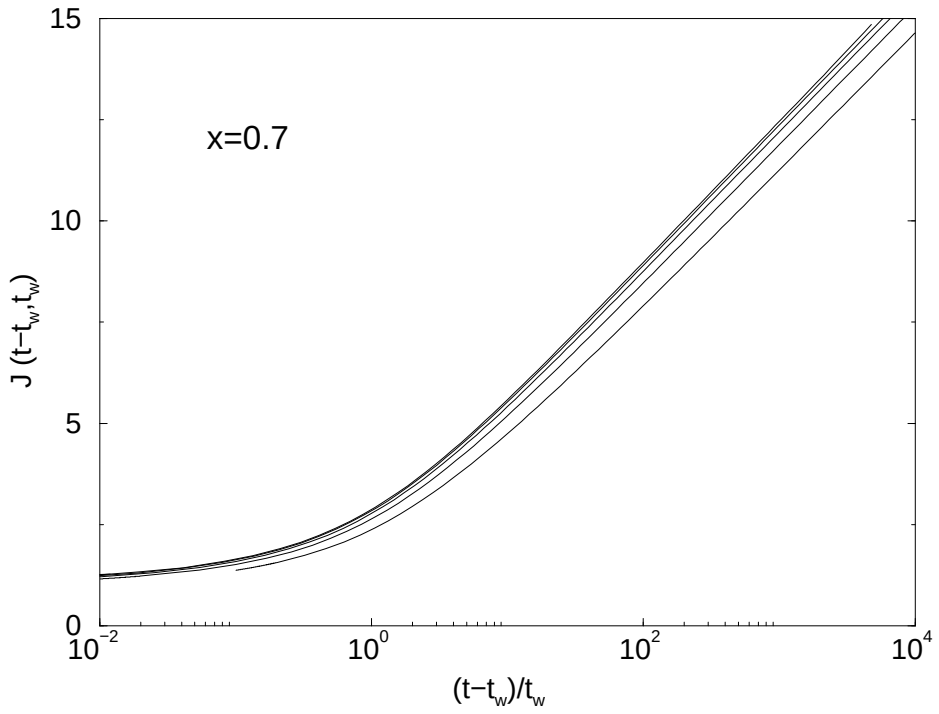

Figure 10: Linear creep compliance $J(t-t_{\rm w},t_{\rm w})$ against scaled time interval $(t-t_{\rm w})/t_{\rm w}$ for noise temperature $x=0.7$. Curves from bottom to top correspond to increasing times $t_{\rm w}=10^2\,,10^3\ldots 10^6$ of stress onset. Note the approach to a limiting scaling form as $t_{\rm w}$ becomes very large compared with the microscopic time $\tau_0=1$.

formally a "small" correction to the leading behavior $\ln(t-t_{\rm w})$. This relatively slight $t_{\rm w}$-dependence in creep measurements is intuitively reasonable: the strain response at time t to step stress is *not* determined purely by the relaxation spectrum at $t_{\rm w}$ (as was the case in step strain, table 1), but by the dynamics of the system over the entire interval between $t_{\rm w}$ and t. This decreases the sensitivity to the time $t_{\rm w}$ at which the perturbation was switched on. Similar remarks hold above the glass point ($1<x<2$): in step strain, we found for $t-t_{\rm w}\gg t_{\rm w}$ a slow transient behavior which depended to leading order upon $t_{\rm w}$ (table 1). For step stress, however, the corresponding $t_{\rm w}$ dependence is demoted to lower order, and the late-time response is dominated by TTI terms.[6] This is visible in Fig. 11. Note that short time and long time behaviors are each independent of $t_{\rm w}$ (as

[6]We restate here why we call these effects for $x>1$ transient behavior rather than ageing. As explained after eq. (19), a consistent definition of long term memory and ageing for the step stress response function $J(t-t_{\rm w},t_{\rm w})$ requires a form of "regularization" by considering the material in question in parallel with a spring of infinitesimal modulus g. This effectively puts an upper limit of $J_{\rm max}=1/g$ on the observable values of $J(t-t_{\rm w},t_{\rm w})$. Taking the limit $t_{\rm w}\to\infty$ for $x>1$ then results in a fully TTI step stress response, whatever the value of $J_{\rm max}$. On the other hand, for $x<1$, the (albeit weak, logarithmic) $t_{\rm w}$-dependence of the response remains visible even for finite values of $J<J_{\rm max}$.

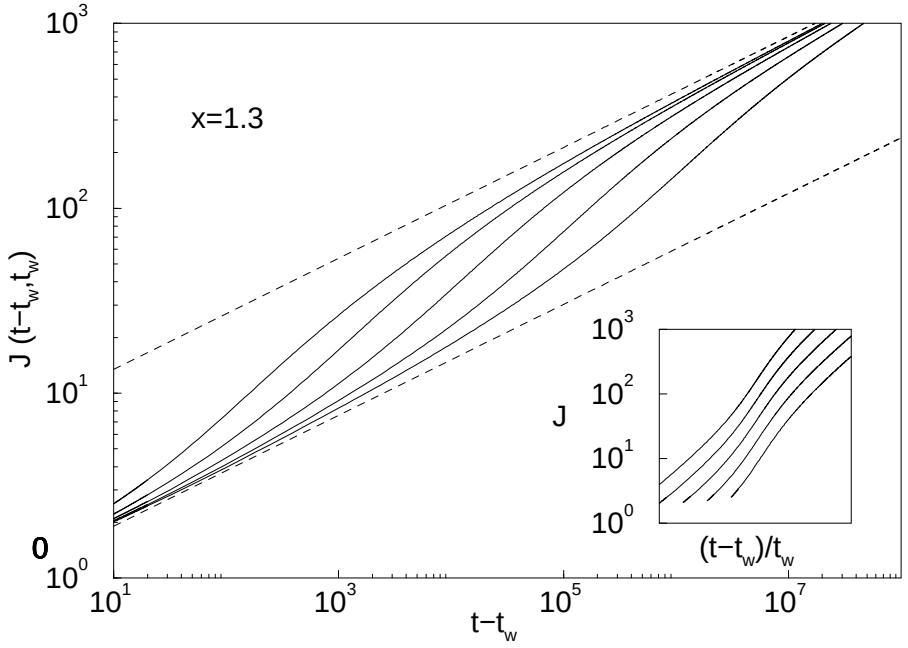

Figure 11: Linear creep compliance $J(t-t_{\rm w},t_{\rm w})$ against time interval $t-t_{\rm w}$ for noise temperature $x=1.3$ for $t_{\rm w}=10^3\,,10^4\ldots10^7$ (solid lines, top to bottom). Lower dashed line: theoretical prediction for the short time regime $t-t_{\rm w}\ll t_{\rm w}$. Upper dashed line: asymptote for long time regime $t-t_{\rm w}\gg t_{\rm w}$. Inset: same data plotted against scaled time $(t-t_{\rm w})/t_{\rm w}$; the order of the curves is reversed.

expected for $x>1$), but that the crossover time between them scales with $t_{\rm w}$ (as shown in the inset).

7.1.2 Oscillatory Stress

For the SGR model it was noted in Sec. 6.1.2 that (*i*) in the oscillatory stress response $G^*(\omega,t,t_{\rm s})$, the $t_{\rm s}$ dependence is negligible for low frequencies ($\omega\ll1$) whenever $\omega(t-t_{\rm s})\gg1$ and $\omega t_{\rm s}\gg1$; (*ii*) these conditions are satisfied in most conventional rheometrical measurements of the viscoelastic spectrum, where an oscillatory strain is maintained for many cycles; and (*iii*), perhaps surprisingly, these facts are true even in the glass phase, $x\leq1$, of the SGR model. We also noted that, because response to oscillatory strain is dominated by memory of the few most recent cycles (over which the system has barely aged), $G^*(\omega,t)$ is the Fourier transform (with respect to the time interval Δt) of the step strain response function $G(\Delta t,t)$ that would be measured if a step strain were applied immediately after the oscillatory measurement had been done; see eq. (45).

We have confirmed numerically that similar remarks apply to the oscillatory stress response function $J^*(\omega,t,t_{\rm s})$. (Although unsurprising, this does require explicit confirmation since, for example, the transient effects from switching on the perturbation could be different in the two cases.) This was defined in Sec. 2.6.2 as the strain response, measured at t, to an oscillatory stress initiated at time $t_{\rm s}$.

Memory of the startup time t_s is indeed small in $J^*(\omega, t, t_s)$ so long as $\omega(t - t_s) \gg 1, \omega t_s \gg 1$ (and $\omega \ll 1$). It appears that, just as in the case of a strain controlled experiment, strain response to oscillatory stress is dominated by memory to the most recent cycles, over which the system has barely aged. We may therefore suppress the t_s parameter, defining a compliance spectrum at time t by $J^*(\omega, t)$. Furthermore, $J^*(\omega, t)$ is found numerically to be the reciprocal of $G^*(\omega, t)$,

$$J^*(\omega, t)G^*(\omega, t) = 1 \tag{52}$$

just as it is (without the t argument) in normal TTI systems. The numerical confirmation of this result is presented in Fig. 12. We emphasize that this result, like the previous one, has been confirmed here specifically for the SGR model; but it may hold more widely for systems with weak long term memory (see Sec. 3).

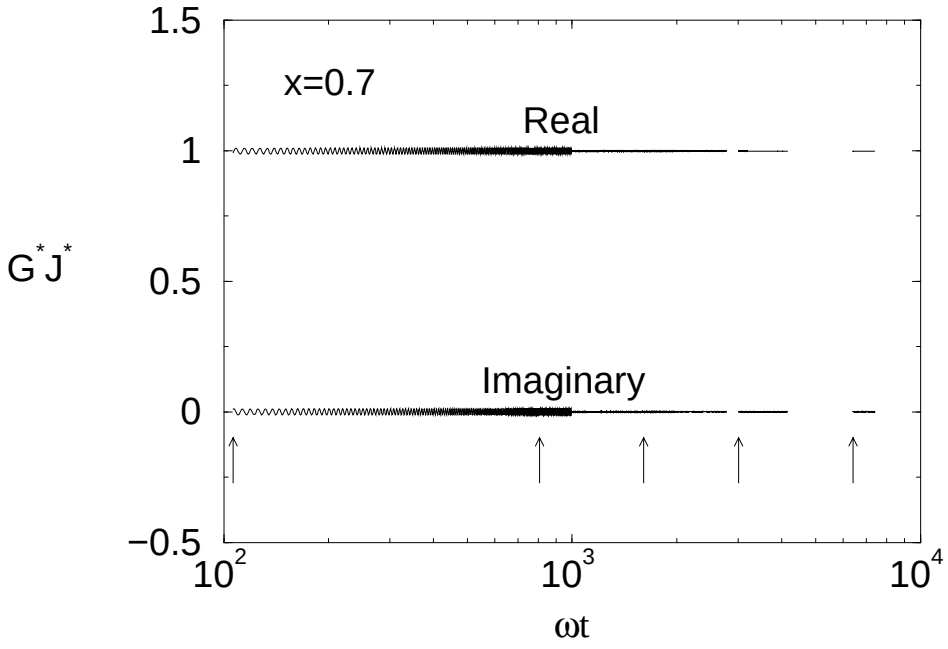

Figure 12: Real and imaginary parts of the product $G^*(\omega, t)J^*(\omega, t)$ vs ωt at noise temperature $x = 0.7$ and frequency $\omega = 0.01$. The usual reciprocity relation between G^* and J^* is seen to hold to within about one percent. Shown are the results of several runs, each over a different time window. A vertical arrow marks the horizontal co-ordinate of the start of each data set. In each run shearing was commenced 20 cycles before the start of data output, to ensure that $\omega(t - t_s) \gg 1$ (necessary for t_s-independence). The oscillatory deviations, visible for the leftmost data set, arise because the other condition for t_s-independence ($\omega t_s \gg 1$) is only just satisfied.

7.2 Nonlinear Response

7.2.1 Step Stress

In Sec. 7.1.1 we argued that a step stress, $\sigma(t) = \sigma_0\Theta(t - t_w)$, of size $\sigma_0 \ll 1$, induces a strain response $\gamma(t)$ which increases over time, but remains linear in σ_0 for at least as long as the linearized constitutive equations predict $\gamma(t) \ll 1$. This is because $\gamma(t)$ provides an upper bound on the local strain of each element. Although sufficient to ensure linearity, this is not always necessary; we require only that the characteristic strain *of those elements which dominate the stress* is small. For $x > 2$ (the Newtonian regime) the dominant elements have lifetimes $O(1)$ and so the response is linear to indefinite times so long as $\sigma_0 \ll 1$ (ensuring $\dot{\gamma}(t) \ll 1$ for all times t). But, whenever $x < 2$, the linear analysis of Sec. 7.1.1 indicates the dominant elements have lifetimes of order $t-t_w$; so a self-consistently linear response is maintained only provided that $\dot{\gamma}(t)(t - t_w) \ll 1$, just as in startup of steady shear (see Sec. 6.2.2; here we make the additional assumption that $\dot{\gamma}$ only changes negligibly between t_w and t). Using the forms for $J(t-t_w, t_w)$ as summarized in table 3, we then find that for $1 < x < 2$ the strain response to step stress remains linear only for as long as $t - t_w \ll (1/\sigma_0)^{1/(x-1)}$. Beyond this time we expect strain-induced yielding to become important.

To confirm the predicted linearity at short times, and to extract the long time nonlinear behavior, we numerically solved the nonlinear constitutive equations (25, 26) by an iterative method (see App. C.2); this was done first for $1 < x < 2$ (Fig. 13). The results show a linear regime of the expected temporal extent, followed by a crossover into a nonlinear steady-state flow regime, in which $\gamma(t) \propto \sigma_0^{1/(x-1)}t$. The latter is in agreement with the flow curve (36).

The same numerical procedure was then used for the glass phase, $x < 1$, for which the flow curve shows a finite yield stress, $\sigma_y(x)$. As expected, the numerical results for step stress of very small amplitude $\sigma_0 \ll \sigma_y$ show no crossover to a steady flow regime at late times. Instead, the system continues to creep logarithmically, according to the linear creep result (table 3):

$$\gamma(t) = \sigma_0 J(t - t_w, t_w) = \sigma_0 \frac{1}{\psi(1) - \psi(x)} \log\left(\frac{t - t_w}{t_w}\right) \tag{53}$$

The resulting value of $\dot{\gamma}(t)(t - t_w)$ never becomes large; so this is self-consistent. Next we studied numerically the case where σ_0 was not small but remained less than the yield stress σ_y. For stresses not too close to the yield stress, we found that the creep was still logarithmic to a good approximation, but now with a nonlinear dependence of its amplitude on stress: $\gamma(t) \approx \sigma_0 A(\sigma_0) J(t - t_w, t_w)$. The prefactor $A(\sigma_0)$ increases rapidly as σ_0 approaches the yield stress σ_y from below. Very close to the yield stress, the creep ceases to be logarithmic; $\gamma(t)$ then grows more quickly, but with a strain rate that still decreases to zero at long times. On the basis of these observations, we suspect that for a given stress σ_0 the creep will be logarithmic for short times (where "short times" might mean the whole time window which is accessible numerically), but will gradually deviate from this for longer times. The deviation is expected to be noticeable sooner for stress values closer to yield. We attempted to verify this conjecture numerically,

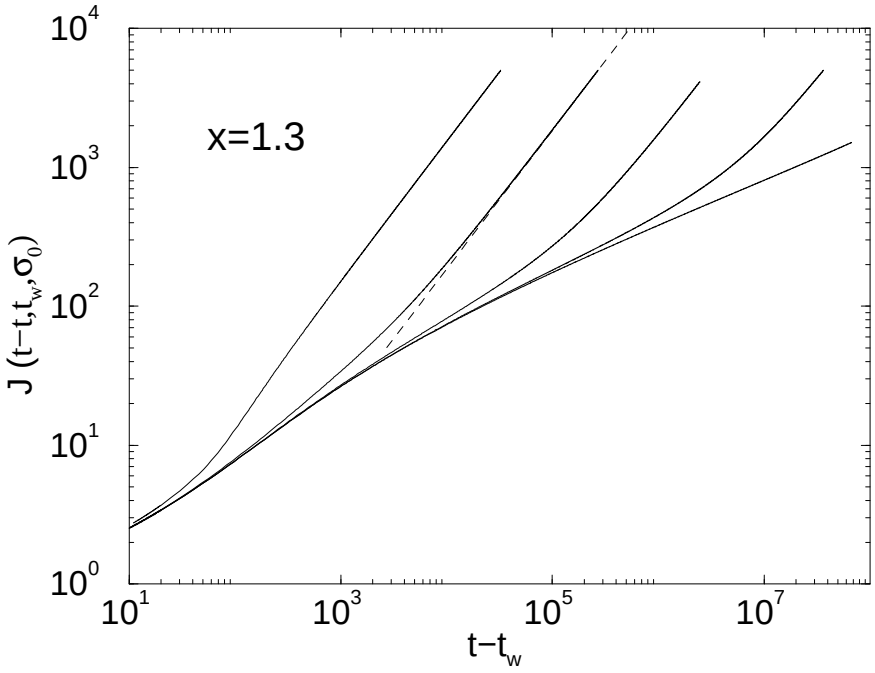

Figure 13: Nonlinear creep compliance $J(t-t_{\rm w}, t_{\rm w}, \sigma_0)$ as a function of time interval $t-t_{\rm w}$, for a step stress of size σ_0 applied at time $t_{\rm w} = 100$. The noise temperature is $x = 1.3$. Solid lines, bottom to top: $\sigma_0 = 10^{-3}, 10^{-2.5}, 10^{-2}, 10^{-1.5}, 10^{-1}$. Over the time intervals shown, the curve for $\sigma_0 = 10^{-3}$ is indistinguishable from the linear compliance (not shown). Dotted line: final flow behavior predicted from steady state flow curve for $\sigma_0 = 10^{-1.5}$.

but were unable to access a large enough range of values of $\ln((t-t_{\rm w})/t_{\rm w})$ to do so. Note that, for any $\sigma_0 < \sigma_{\rm y}$, the system ages indefinitely, and there is no approach to a regime of steady flow.

Finally, as expected from the flow curve, only for stress amplitudes exceeding the yield stress $\sigma_{\rm y}$ (which of course depends on x) did we see an eventual crossover from logarithmic creep to steady flow at long times; when that happened, we recovered numerically the flow-curve result, $\gamma(t) \propto (\sigma_0 - \sigma_{\rm y})^{1/(1-x)}(t-t_{\rm w})$. Fig. 14 shows examples of our numerical results that illustrate the various features of nonlinear creep in the glass phase mentioned above. (Note that whereas for most other shear scenarios we chose to present glass phase results for a noise temperature $x = 0.7$, we here took $x = 0.3$. The yield stress is larger at this value of x, giving us a larger window $0 < \sigma_0 < \sigma_{\rm y}$ over which we see ageing and creep uninterrupted by a crossover into flow.) Comparison of the curves for the two different waiting times for $\sigma_0/\sigma_{\rm y} = 1.2$ shows that before the crossover into flow, the response scales with $(t-t_{\rm w})/t_{\rm w}$; once ergodicity has been restored and the system flows, on the other hand, scaling with $t-t_{\rm w}$ is recovered.

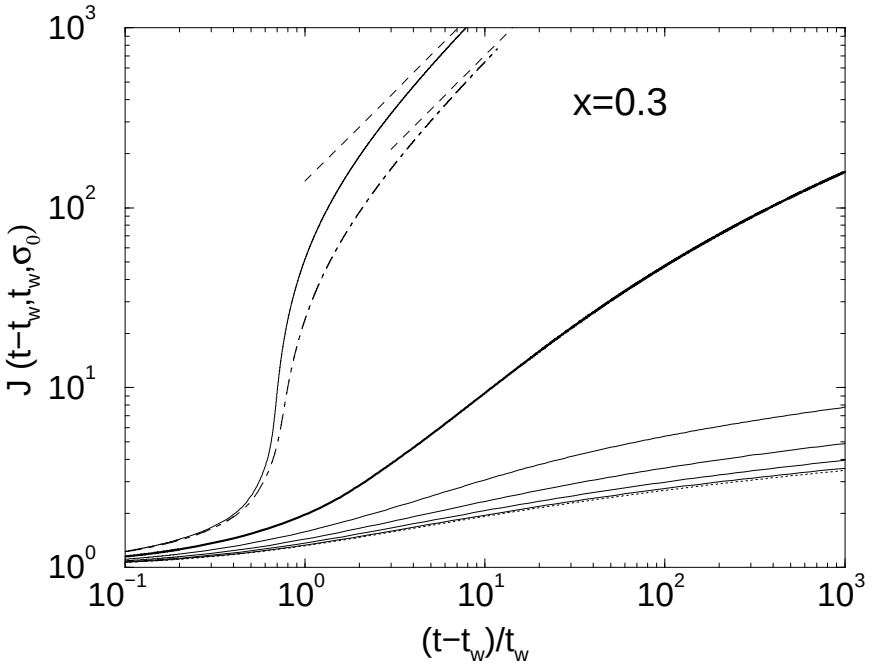

Figure 14: Nonlinear creep compliance $J(t-t_{\rm w},t_{\rm w},\sigma_0)$ as a function of scaled time interval $(t-t_{\rm w})/t_{\rm w}$, for a step stress of size σ_0 applied at time $t_{\rm w}$. The noise temperature is $x=0.3$. Solid curves, bottom to top: $\sigma_0/\sigma_{\rm y}=0.2\,,0.4,\ldots,1.2$, all for $t_{\rm w}=100$. The case $\sigma_0=\sigma_{\rm y}$ is shown in bold; the dotted curve is the linear response result ($\sigma_0\to 0$). The dot-dashed curve shows the effect of decreasing the waiting time to $t_{\rm w}=50$, for $\sigma_0/\sigma_{\rm y}=1.2$. The dashed lines are the predictions for final flow behavior (for the stress above yield) from the steady state flow curve.

8 Conclusion

In this paper we studied theoretically the role of ageing in the rheology of soft materials. We first provided, in Sec. 2 a general formulation of the linear and nonlinear rheological response functions suited to samples that show ageing, in which time translation invariance of material properties is lost. (Our analysis extends and, we hope, clarifies that of Struik (1978).) This was followed in Sec. 3 by a review of the concept of ageing, formally defined by the presence of long term memory, which can be either weak or strong. We suggested that for many rheological applications the main interest is in systems with weak long term memory: these have properties that are age-dependent, but not influenced by perturbations of finite duration that occurred in the distant past. We conjectured that weak long term memory is sufficient to cause the age-dependent linear viscoelastic modulus to become independent of the start time $t_{\rm s}$ of the oscillatory shear ($G^*(\omega,t,t_{\rm s})\to G^*(\omega,t)$) while retaining a dependence on system age t; for it to then obey the usual Fourier relation with the linear step strain response (likewise dependent on age $t_{\rm w}$); and for it to obey a reciprocal relation $G^*(\omega,t)J^*(\omega,t)=1$ with the time-varying compliance, similarly defined. Pending a general proof of

these conjectures, all such relationships between age-dependent rheological quantities do however require empirical verification for each experimental system, or theoretical model, that one studies.

Within this conceptual framework, we then explored rheological ageing effects in detail for the SGR model. After reviewing the basic rheological definition of the model in Sec. 4, we discussed in Sec. 5 its ageing properties from the point of view of the mean jump rate $Y(t)$ whose behavior is radically different in the glass phase (noise temperature $x < 1$) from that in the normal phase ($x > 1$). The glass phase of the SGR model is characterized by "weak ergodicity breaking", which means that the elastic elements that it describes evolve forever towards higher yield thresholds (deeper traps), causing a progression toward more elastic and less lossy behavior. Within the glass phase, there is a yield stress $\sigma_{\rm y}$, and for applied stresses less than this, genuine ageing effects arise. These phemonena were explored in depth in Sec. 6 and Sec. 7 for the cases of imposed stress and imposed strain respectively. Ageing effects are distinguished from otherwise similar transient phenomena (arising, for example, when $x > 1$) by the criterion that a significant part of the stress relaxation, following infinitesimal step strain, occurs on timescales that diverge with the age of the system at the time of strain application. This rheological definition appears appropriate for most soft materials and follows closely the definition of long-term memory in other areas of physics (Cugliandolo and Kurchan, 1995; Bouchaud et al., 1998; Cugliandolo and Kurchan, 1993).

In the glass phase of the SGR model, the nature of the ageing is relatively simple; for a step strain or stress applied at time $t_{\rm w}$, both the linear stress relaxation function $G(t - t_{\rm w}, t)$ and the linear creep compliance $J(t - t_{\rm w}, t_{\rm w})$ become functions of the scaled time interval $(t - t_{\rm w})/t_{\rm w}$ only. This scaling is a simple example of the 'time waiting-time superposition' principle postulated empirically by Struik (1978) (in the somewhat different context of glassy polymers). The time-dependent viscoelastic spectra $G'(\omega, t)$ and $G''(\omega, t)$ have the characteristic ageing behavior shown in Fig. 1: a loss modulus that rises as frequency is *lowered*, but falls with age t, in such a way that it always remains less than $G'(\omega, t)$ (which is almost constant by comparison). For $x < 1$ such spectra collapse to a single curve (see Fig. 8) if ωt, rather than ω, is used as the independent variable. Note that in more complicated systems, Eq. (20) may be required instead, to describe ageing on various timescales that show different divergences with the sample age $t_{\rm w}$. (Even in simple materials, there may be an additional non-ageing contribution to the stress relaxation which the SGR model does not have; this will also interfere with the scaling collapse of both $G(t - t_{\rm w}, t_{\rm w})$ and $G^*(\omega, t)$.) We found that, in its glass phase, the SGR model has weak long term memory, and we confirmed numerically that the conjectured relationships, Eqs. (12,13,14), among age-dependent linear rheological quantities indeed hold in this case.

Significant ageing was also found for nonlinear rheological responses of the SGR model. For example the nonlinear step-strain relaxation follows the same ageing scenario as the linear one, except that all relaxation rates are speeded up by a single strain-dependent factor (Eq. (50)). This form of nonlinearity is a characteristic simplification of the SGR model, and would break down if the elastic elements in the model were not perfectly Hookean between yield events.

Another interesting case was startup of steady shear; here there is no significant ageing in either the initial (elastic) or the ultimate (steady flow) regime; yet, as shown in Fig. 9, the intermediate region shows an overshoot that is dependent on sample age. For an old sample, the elastic elements have higher yield thresholds. The elastic regime therefore extends further before the imposed strain finally causes yielding, followed by a larger drop onto the same steady-shear plateau. The plateau itself is age-independent: the presence of a finite steady flow rate, but not a finite stress, is always enough to interrupt the ageing process within the SGR model. Finally we found that the nonlinear creep compliance (Fig. 14), shows interesting dependence on both the stress level and the age of the sample; for small stresses we found logarithmic creep (for all $x < 1$), crossing over, as the yield stress is approached, to a more rapid creep that nonetheless appears to have zero strain rate in the long time limit. Nonlinear creep gives challenging computational problems in the SGR model, which is otherwise simple enough, as we have shown, that almost all its properties can be calculated either by direct asymptotic analysis or using (relatively) standard numerics. Remaining drawbacks include (from a phenomenological viewpoint) the lack of tensorial elasticity in the model and (from a fundamental one) uncertainty as to the proper physical interpretation, if one indeed exists, of the noise temperature x (Sollich et al., 1997; Sollich, 1998).

Though obviously oversimplified, the SGR model as explored in this paper may provide a valuable paradigm for the experimental and theoretical study of rheological ageing phenomena in soft solids. More generally, the conceptual framework we have presented, which closely follows that developed to study ageing in non-flowing systems such as spin-glasses, should facilitate a quantitative analysis of rheological ageing phenomena across a wide range of soft materials.

A Calculation of Linear Response Properties

A.1 Initial Condition

In discussing the SGR model's non-equilibrium behavior (Secs. 6 and 7) we considered for definiteness a system prepared by a quench from an infinite noise temperature (see Sec. 5.1), *i.e.*, with an initial distribution $P_0(E) = \rho(E)$ of yield energies or trap depths. For our predictions to be easily compared to experimental data, however, they must be largely independent of the details of sample preparation. To test for such independence, we consider the extent to which our results would change if the pre-quench temperature, which we denote by x_0, were finite. This corresponds to an initial trap depth distribution

$$P_0(E) \propto \exp(E/x_0)\rho(E) \tag{54}$$

In this appendix, we restrict ourselves to the linear response regime, where the effects of finite x_0 (if any) are expected to be most pronounced; nonlinearity tends to eliminate memory effects. The same is true for high temperatures, and correspondingly we will find that the influence of x_0 on our results is confined mainly to final (post-quench) temperatures x within the glass phase ($x < 1$).

A.2 Yield Rate

The yield or hopping rate is the basic quantity from which other linear response properties can be derived; see eqs. (39,42,51). It can be calculated from the second constitutive equation (26)

$$1 = G_0(t) + \int_0^t Y(t')G_\rho(t-t')dt' \tag{55}$$

where we have replaced $Z(t,t')$ by $t-t'$, as is appropriate in the linear response regime. The function $G_0(t)$ is defined in (28); for the initial condition (54) it is related to G_ρ via

$$G_0(t) = G_\rho(t,y), \qquad y = x(1-1/x_0)$$

where we have now included explicitly the noise temperature argument (y) in the argument list of G_ρ. Substituting this into (55), and taking Laplace transforms with λ as our reciprocal time variable, we get:

$$\frac{1}{\lambda} = \bar{G}_\rho(\lambda,y) + \bar{Y}(\lambda)\bar{G}_\rho(\lambda,x) \tag{56}$$

and hence

$$\bar{Y}(\lambda) = \frac{\frac{1}{\lambda} - \bar{G}_\rho(\lambda,y)}{\bar{G}_\rho(\lambda,x)} \tag{57}$$

in which (taking Laplace transforms of (28))

$$\bar{G}_\rho(\lambda,x) = x\int_1^\infty \frac{\tau^{-x-1}}{\lambda+\tau^{-1}}\,d\tau = x\int_1^\infty \frac{\tau^{-x}}{1+\lambda\tau}\,d\tau \tag{58}$$

In its present form (57) cannot be inverted analytically. We will focus on the long time regime, however, where progress can be made by using an alternative expression for $\bar{G}_\rho$. From (58), $\bar{G}_\rho(\lambda,x)$ has poles at $\lambda = -\tau^{-1}$. Because of the integration over all $\tau = 1\ldots\infty$, these poles combine into a branch cut singularity on the (negative) real axis between $\lambda = -1$ and $\lambda = 0$. We will now derive an expression for $\bar{G}_\rho$ that is valid near this branch cut. This expression does introduce spurious singularities on the negative real axis for $\lambda < 1$. But after inversion of the Laplace transform these only give contributions to $G_\rho(t)$ decaying exponentially or faster in t; they can therefore be ignored in the long-time limit. We first write (58) as

$$\frac{1}{x}\,\bar{G}_\rho(\lambda,x) = \int_0^\infty \frac{\tau^{-x}}{1+\lambda\tau}\,d\tau - \int_0^1 \frac{\tau^{-x}}{1+\lambda\tau}\,d\tau \tag{59}$$

After the rescaling $\lambda\tau \to \tau$, the first term becomes a representation of the Beta function. (The rescaling can be carried out only when λ is real and positive. But by analytic continuation, the result (60) also holds for complex λ outside the branch cut of λ^{x-1}, *i.e.*, everywhere except on the negative real axis.) In the second term, because now $\tau \le 1$, we can expand the denominator into a series that is convergent for $|\lambda| < 1$. This gives the desired expression

$$\bar{G}_\rho(\lambda,x) = a(x)\lambda^{x-1} + \sum_{n=0}^{\infty} b_n(x)\lambda^n \tag{60}$$

in which

$$a(x) = x\Gamma(x)\Gamma(1-x), \qquad b_n(x) = \frac{x(-1)^{n+1}}{n+1-x} \tag{61}$$

This is valid for $|\lambda| < 1$ and therefore in particular near the branch cut $\lambda = -1 \ldots 0$; in the representation (60), this branch cut is apparent in the fractional power of λ in the first term. The above derivation applies a priori only for $x < 1$, because otherwise the integrals in (59) diverge at the lower end. However, using the relation

$$\frac{1}{x+1}\,\bar{G}_\rho(\lambda, x+1) = \frac{1}{x} - \frac{\lambda}{x}\,\bar{G}_\rho(\lambda, x)$$

which follows directly from (58), it can easily be shown that (60) holds for all x. (For integer x, there are separate singularities in the first and second term of (60), but these just cancel each other.)

We can now substitute (60,61) into (57) and expand the denominator to find a readily invertible expression for $\bar{Y}(\lambda)$. Clearly the manner in which we perform the expansion depends on whether $x > 1$ or $x < 1$. Abbreviating $a(x) = a$, $a(y) = a'$, and $b_n(x) = b_n$, we have for $x > 1$:

$$\bar{Y}(\lambda) = \frac{1}{\lambda}\left[\frac{1}{b_0} - \frac{a}{b_0^2}\lambda^{x-1} - \frac{a'}{b_0}\lambda^y + O\left(\lambda^{2(x-1)}, \lambda^{y+x-1}, \lambda, \ldots\right)\right]$$

which, upon inversion of the Laplace transform, gives:

$$Y(t) = \frac{1}{b_0} - \frac{1}{\Gamma(2-x)}\frac{a}{b_0^2}t^{1-x} - \frac{1}{\Gamma(1-y)}\frac{a'}{b_0}t^{-y} + O\left(t^{2(1-x)}, t^{1-x-y}, \ldots\right) \tag{62}$$

the first term of which is the asymptotic expression for $Y(t)$ above the glass points, as in (37). For $x < 1$ on the other hand, we have

$$\bar{Y}(\lambda) = \frac{1}{\lambda}\left[\frac{\lambda^{1-x}}{a} - \frac{b_0\lambda^{2(1-x)}}{a^2} - \frac{a'}{a}\lambda^{y+1-x} + O\left(\lambda^{3(1-x)}, \lambda^{y+2(1-x)}, \ldots\right)\right] \tag{63}$$

which can be inverted to give

$$Y(t) = \frac{1}{\Gamma(x)}\frac{t^{x-1}}{a} - \frac{1}{\Gamma(1+2(x-1))}\frac{b_0 t^{2(x-1)}}{a^2} - \frac{a'}{a\Gamma(x-y)}t^{x-1-y} + O\left(t^{3(x-1)}, t^{2(x-1)-y}\right) \tag{64}$$

the first term again being in agreement with (37). Finally, to obtain $Y(t)$ *at* the glass point $x = 1$ we rewrite (63) as:

$$\bar{Y}(\lambda) = -\frac{1}{b_0\lambda}\left[\sum_{n=1}^{p} z^n(\lambda) + O\left(\lambda^y, \lambda, \lambda^{(p+1)(1-x)} \ldots\right)\right]$$

in which $z(\lambda) = -b_0\lambda^{1-x}/a$ and p is the largest integer which is less than $1/(1-x)$. Inversion of the Laplace transform gives

$$Y(t) = \frac{-1}{b_0}\sum_{n=1}^{p}\frac{z^n(t)}{\Gamma(1+n(x-1))} + O\left(t^{-y}, t^{(p+1)(x-1)}, \ldots\right)$$

in which $z(t) = -b_0 t^{x-1}/a$. The Gamma function can now be expanded around $\Delta = 1 - x = 0$; the sum over p can be performed explicitly for each term in this expansion. Retaining only the dominant terms for small Δ, and also taking the limit $\Delta \to 0$ of the quantities $z(t)$, a and b_0, one finds eventually

$$\lim_{x\to 1} Y(t) = \frac{1}{\ln(t)} + \frac{\Gamma'(1)}{\ln^2(t)} + O\left(\frac{1}{\ln^3(t)}\right)$$

as stated in (37).

Consider now the effect of the pre-quench temperature x_0 on the above results for the asymptotic behavior of the hopping rate $Y(t)$. We note first that all the leading terms are independent of y and hence of x_0. For $x > 1$, the largest y-dependent subleading term (t^{-y}) in (62) becomes more important for smaller pre-quench temperatures x_0. However, provided we restrict ourselves to the regime $x_0 > x$ (*i.e.*, to a non-equilibrium situation in which a quench is actually performed; $x = x_0$ corresponds to equilibrium conditions), we see that $y > x - 1$ and that, even to subleading order, $Y(t)$ is independent of x_0. (We note furthermore that in the case of the deep quench defined in Sec 5.1, $y = x$ and the term t^{-y} is very small.) For $x < 1$, in (64), the relative importance of the largest y-dependent term (t^{x-1-y}) again depends upon the relative values of the pre- and post-quench temperatures. For a high enough pre-quench temperature (specifically, provided $y > 1 - x$, *i.e.*, provided $x_0 > x/(2x-1)$) the leading and subleading terms of $Y(t)$ are independent of x_0. For any post-quench temperature $x < 1/2$, the subleading term necessarily depends upon x_0 since the condition defined above for independence cannot be satisfied. Intuitively this is physically reasonable, since in general we expect a system at a lower temperature to remember its initial condition more strongly.

A.3 Step Strain and Oscillatory Strain Response

Once the yield rate $Y(t)$ is known, the linear stress response $G(t-t_\mathrm{w}, t_\mathrm{w})$ to a step strain can be calculated from (39). To get its asymptotic behavior for $t - t_\mathrm{w} \gg 1$, $t_\mathrm{w} \gg 1$, the two regimes in which the time interval $t - t_\mathrm{w}$ is much less and much greater than the age at the time of stress application t_w have to be considered separately. In the first regime ($t - t_\mathrm{w} \ll t_\mathrm{w}$), one can Taylor expand the hopping rate Y around its value at time t. In the second regime, we rewrite (39) as

$$G(t - t_\mathrm{w}, t_\mathrm{w}) = G_0(t) + \int_0^{t_\mathrm{w}} Y(t') G_\rho(t - t') dt' \tag{65}$$

The first term on the right-hand side can then be shown to be subdominant (at least for $x_0 \to \infty$; see Sec. A.4 below), and the second can be treated by expanding $G_\rho(t - t')$ around $t' = 0$. To leading order, one then finds the results in table 1. The asymptotic behavior of the stress response to oscillatory strain, $G^*(\omega, t, t_\mathrm{s})$, is obtained in a similar manner from (42).

A.4 Rheological Irrelevance of Initial Condition

In App. A.2 we discussed the influence of the initial state of the sample, as parameterized by the "pre-quench" temperature x_0, on the yield rate $Y(t)$. Now

we consider the effects of x_0 on the various (linear) rheological observables, concentrating on the regime $x < 1$ where such effects are expected to be most pronounced. We begin with the response to a step strain, $G(t-t_\mathrm{w}, t_\mathrm{w})$. In the short time regime $t-t_\mathrm{w} \ll t_\mathrm{w}$, it follows directly from (39) that x_0 affects only subdominant terms (through its effect on $Y(t)$). In the long time regime $t-t_\mathrm{w} \gg t_\mathrm{w}$, we see similarly from (65) that any effect on the leading behavior can only be through the first term on the right-hand side, $G_0(t) = G_\rho(t,y) \sim t^{-y}$. Comparing this with the second term, which from table 1 is of order $(t_\mathrm{w}/t)^x$ (note that $t \approx t-t_\mathrm{w}$ in the long time regime), and using $y = x(1-1/x_0)$, one finds that the effect of x_0 is negligible up to $t \approx t_\mathrm{w}^{x_0}$. For larger t, $G(t-t_\mathrm{w}, t_\mathrm{w}) \approx G_0(t) \approx G_0(t-t_\mathrm{w})$ and the response is TTI to leading order. An intuitive explanation for this behavior can be found by analysing the evolution of the relaxation time distribution $P(\tau, t_\mathrm{w})$ with t_w. It can be shown that the initial condition $P(\tau, 0)$ is remembered in the long time tail of this distribution, $\tau \gg t_\mathrm{w}^{x_0}$. For times $t \gg t_\mathrm{w}^{x_0}$, these long relaxation times dominate the behavior of $G(t-t_\mathrm{w}, t_\mathrm{w})$ and cause the observed x_0-dependence.

For the step stress response $J(t-t_\mathrm{w}, t_\mathrm{w})$, we found in Sec. 7.1.1 that memory effects are rather weaker than for the step strain response. This is because J is sensitive to the average behavior of the relaxation time distribution $P(\tau, t')$ over the time interval $t' = t_\mathrm{w} \ldots t$, while G depends on $P(\tau, t_\mathrm{w})$ only. Correspondingly, we also find that $J(t-t_\mathrm{w}, t_\mathrm{w})$ is affected only weakly by the initial preparation of the system and hence by x_0. All effects are in subdominant terms; for the long time behavior in the glass phase, for example, one finds that the asymptotic behavior $J(t-t_\mathrm{w}, t_\mathrm{w}) \sim \ln((t-t_\mathrm{w})/t_\mathrm{w})$ is only changed by an x_0-dependent constant offset.

Finally, consider the oscillatory response functions $G^*(\omega, t, t_\mathrm{s})$ and $J(\omega, t, t_\mathrm{s})$. Any linear oscillatory perturbation effectively probes only those traps which have a relaxation time $\tau < 1/\omega$. Provided such traps have attained an x_0-independent distribution by the time the perturbation is switched on at t_s, $G^*(\omega, t, t_\mathrm{s})$ and $J^*(\omega, t, t_\mathrm{s})$ will be insensitive to x_0. It can be shown that the requirement for this is $\tau \ll t_\mathrm{s}^{x_0}$ for all $\tau < 1/\omega$ and hence $\omega t_\mathrm{s}^{x_0} \gg 1$. We argue in App. B, however, that in order to get a sensible measurement of G^* (and J^*) which is independent of *start time* t_s, we must ensure $\omega t_\mathrm{s} \gg 1$. This condition then automatically guarantees that the results are independent of x_0.

In summary, the only significant effects of the initial sample preparation appear in the step strain response at long times ($t \gg t_\mathrm{w}^{x_0}$). In the other linear response properties that we studied, the initial condition only affects subdominant terms. We reiterate our earlier statement that for nonlinear response, the initial sample condition should be even less important, because nonlinearities tend to wipe out memory effects. Finally, we mention the work of Kob and Barrat (1997), who investigated the effects of pre-quench temperature in a Lennard-Jones glass using computer simulations. They rationalized their data by the hypothesis that different pre-quench temperatures introduce different offsets in the effective age of the sample. Since these offsets are finite, this suggests asymptotic behavior for large t_w which is independent of pre-quench temperature, in qualitative agreement with our findings for the SGR model.

B Irrelevance of Switch-on Time in the Glass Phase

It was stated in Sec. 6.1.2 that $G^*(\omega, t, t_s)$ does not depend on t_s so long as $\omega(t-t_s) \gg 1$ and $\omega t_s \gg 1$. These criteria do not depend on the noise temperature x, and therefore hold even in the glass phase, $x \leq 1$, where ageing occurs.

This behavior can be understood as follows. Consider a material which has not been strained since preparation except during a time window of duration t^* before the present time t. First write the linearized constitutive equation as:

$$\sigma(t) = -\int_{t-t^*}^{t} \gamma(t') \frac{dG(t-t',t')}{dt'} dt' \tag{66}$$

where, for the SGR model

$$\frac{dG(t-t',t')}{dt'} = -\delta(t-t') + Y(t')G_\rho(t-t') \tag{67}$$

with $G_\rho(t-t') \sim (t-t')^{-x}$. This result follows by differentiation of (39), respecting the fact that $G(t-t_w, t_w)$ vanishes for negative $t-t_w$ (that is, it contains a factor $\Theta(t-t_w)$ which is conventionally suppressed).

Now consider the case of a step strain imposed at $t-t^*$, so that $\gamma(t)$ is constant in (66). Because dG/dt' contains a contribution of order $(t-t')^{-x}$, the integral has significant contributions from t' near $t-t^*$ whenever $x \leq 1$; in fact in the absence of the factor $Y(t')$ the integral would not even converge to a finite limit as t^* becomes large. This is a signature of long-term memory: Even the strain history in the distant past has an effect on the stress at time t. On the other hand, for an oscillatory strain (likewise switched on at $t-t^*$) one has (66) with $\gamma(t) = \gamma_0 e^{i\omega t}$, and even without the factor $Y(t')$ the integral would now converge to a finite limit so long as ωt^* is large. The convergence of the oscillatory integral follows from the mathematical result known as Jordan's lemma (Copson, 1962) which, crudely speaking, states that inserting the oscillatory factor $e^{i\omega t'}$ has a similar effect to converting the integrand, dG/dt', to $\omega d^2G/dt'^2$. (Physically, this extra time derivative arises since the stress at t due to any previously executed strain cycle must involve the change in dG/dt' over the cycle: if this change is small, the response to positive and negative strains will cancel.) Accounting for this extra time derivative, it is simple to check that the most recently executed strain cycles indeed dominate the response at time t, in contrast to the non-oscillatory case where the entire strain history contributes.

This observation allows us to simplify (66) further by setting $G(\Delta t, t') \to G(\Delta t, t)$ where $\Delta t = t - t'$ (we assume $\omega t \gg 1$, so that the variation in the stress response function over a fixed number of recent cycles is negligible). Likewise, the limit of integration can safely be set to $\Delta t = \infty$. Thus we have

$$G^*(\omega, t) = \int_0^\infty e^{-i\omega\Delta t} \frac{dG(\Delta t, t)}{d\Delta t} d\Delta t \tag{68}$$

This can be integrated by parts to give (45) as required.

C Numerical Methods

C.1 Yield Rate in the Linear Regime

To obtain numerical results for the linear response properties of the SGR model, the yield rate $Y(t)$ has to be calculated first. A convenient starting point for this can be obtained by differentiating (55):

$$Y(t) = -G_0'(t) - \int_0^t Y(t')G_\rho'(t-t')\,dt' \tag{69}$$

This is a Volterra integral equation of the second kind, which can in principle be solved by standard numerical algorithms (Press et al., 1992). Such algorithms are based on discretizing the time domain into a grid $t_0 = 0, t_1 \ldots t_n$; the values $Y_n = Y(t_n)$ are then calculated successively, starting from the known value of Y_0. The subtlety in our case is the choice of the grid: Because for times $t \gg 1$ we expect the hopping rate to be a power law, we expect relative discretization errors given a time-step Δt to scale as $\Delta t/t_n$. Once we have chosen an acceptable (constant) value for the discretization error we are therefore at liberty to increase the time-step Δt linearly with the time t_n, which corresponds to using a geometric time grid. This allows us to generate data over many decades without too much computational effort. To improve accuracy, we also used a spline interpolation between the known points $(t_0, Y_0), (t_1, Y_1) \ldots (t_{n-1}, Y_{n-1})$ when determining the next value Y_n.

C.2 Strain Response to Finite Step Stress

The numerical scheme used to solve (25) and (26) in the case of an imposed step stress $\sigma(t) = \sigma_0\Theta(t - t_\mathrm{w})$ is rather more complicated. This is because both the strain and the hopping rate, which are coupled through nonlinear integral equations, have to be calculated as functions of time. Again, we discretize time into a grid $t_0, t_1 \ldots t_n$, where $t_0 = t_\mathrm{w}^+$, and proceed along the grid calculating the strain γ_n and the hopping rate Y_n for successive values of the index n.[7] The first data point $\gamma_0 = \gamma(t_\mathrm{w}^+)$ and $Y_0 = Y(t_\mathrm{w}^+)$ on this grid is obtained directly by treating the discontinuity at t_w "by hand". At any subsequent time-step the two nonlinear constitutive equations (25) and (26) are solved simultaneously. The first is essentially of the form:

$$0 \;=\; f(\gamma_n, Y_n, \{\gamma_{n'}\}, \{Y_{n'}\}, t_\mathrm{w}, \sigma_0) \quad \text{for} \quad 0 \le n' < n \tag{70}$$

while the second can be differentiated and rearranged to give

$$Y_n \;=\; g(\gamma_n, \{\gamma_{n'}\}, \{Y_{n'}\}, t_\mathrm{w}, \sigma_0) \quad \text{for} \quad 0 \le n' < n \tag{71}$$

Because (70) cannot be solved explicitly for γ_n, we use an iterative process. At each time-step we start by placing sensible upper and lower bounds on γ_n, derived

[7] Note that the integral form of the constitutive equations renders the strain and the hopping rate at any time step t_n dependent upon the values of these quantities at all previous times – even times prior to stress application ($0 < t' < t_\mathrm{w}$). However, for such times the strain is clearly zero and the hopping rate is identical to that in the linear response regime, calculated previously.

from physical expectations about the time dependence of the strain $\gamma(t)$. Each bound in turn is substituted into (71) (to find the corresponding value of Y_n) and (with its Y_n) into the function f of the right hand side of (70). The secant method (Press et al., 1992) is then used to update one of the bounds, and the new bound used to calculate a new Y_n and f. This process is repeated until we obtain a sufficiently small value of f ($|f| < 10^{-8}$). The current values of γ_n and Y_n are then accepted and we proceed to the next time-step.

We initially chose a geometric grid of time values $t_0, t_1 \ldots$, but this led to numerical instabilities. We therefore switched to an adaptive procedure which chooses time-steps such that the strain always increases by approximately the same amount in a given time-step.

Finally, note that at each iteration loop of each time-step we in principle need to evaluate double integrals of the form $I = \int_0^t h(Z(t,t'))dt'$ in which

$$Z(t,t') = \int_{t'}^{t} dt'' \exp\{[\gamma(t'') - \gamma(t')]^2/2x\} \tag{72}$$

Because this is very costly computationally, we first calculate at each loop $Z(t,t')$ on a grid of t' values ranging from 0 to t and set up an interpolation over the calculated points. We are then left with single integrals of the same form as I, and look up the value of Z whenever the integrand is called.

References

H A Barnes, J F Hutton, and K Walters. *An introduction to rheology.* Elsevier, Amsterdam, 1989.

B Bernstein, E A Kearsley, and L J Zapas. A study of stress relaxation with finite strain. *Trans. Soc. Rheol.*, 7:391–410, 1963.

J P Bouchaud. Weak ergodicity breaking and aging in disordered-systems. *J. Phys. (France) I*, 2(9):1705–1713, 1992.

J P Bouchaud, L F Cugliandolo, J Kurchan, and M Mézard. Out of equilibrium dynamics in spin-glasses and other glassy systems. In A P Young, editor, *Spin glasses and random fields*, Singapore, 1998. World Scientific.

J P Bouchaud and D S Dean. Aging on Parisis tree. *J. Phys. (France) I*, 5(3): 265–286, 1995.

M E Cates and S J Candau. Statics and dynamics of wormlike surfactant micelles. *J. Phys. Cond. Matt.*, 2:6869–6892, 1990.

M Cloître, 1999. Laboratoire Mixte CNRS/Elf-Atochem, Levallois-Perret, France. Private communication.

E T Copson. *An introduction to the theory of functions of a complex variable.* Oxford University Press, New York, 1962.

L F Cugliandolo and J Kurchan. Analytical solution of the off-equilibrium dynamics of a long- range spin-glass model. *Phys. Rev. Lett.*, 71(1):173–176, 1993.

L F Cugliandolo and J Kurchan. On the out-of-equilibrium relaxation of the Sherrington- Kirkpatrick model. *J. Phys. A*, 27(17):5749–5772, 1994.

L F Cugliandolo and J Kurchan. Weak ergodicity breaking in mean-field spin-glass models. *Phil. Mag. B*, 71(4):501–514, 1995.

L F Cugliandolo, J Kurchan, P LeDoussal, and L Peliti. Glassy behaviour in disordered systems with nonrelaxational dynamics. *Physical Review Letters*, 78(2):350–353, 1997a.

L F Cugliandolo, J Kurchan, and L Peliti. Energy flow, partial equilibration, and effective temperatures in systems with slow dynamics. *Phys. Rev. E*, 55 (4):3898–3914, 1997b.

E Dickinson. *An introduction to food colloids.* Oxford University Press, Oxford, 1992.

M Doi and S F Edwards. *The Theory of Polymer Dynamics.* Clarendon Press, Oxford, 1986.

R M L Evans, M E Cates, and P Sollich. Diffusion and rheology in a model of glassy materials. *European Physical Journal B*, 10:705–718, 1999.

R Gardon and O S Narayanaswamy. Stress and volume relaxation in annealing flat glass. *J. Am. Cer. Soc.*, 53:380–385, 1970.

I M Hodge. Physical aging in polymer glasses. *Science*, 267(5206):1945–1947, 1995.

H. Hoffmann and A. Rauscher. Aggregating systems with a yield stress value. *Coll. Polymer Sci.*, 271(4):390–395, 1993.

S D Holdsworth. Rheological models used for the prediction of the flow properties of food products. *Trans. Inst. Chem. Eng.*, 71(C):139–179, 1993.

L L Hopkins. Stress relaxation or creep of linear viscoelastic substances under varying temperature. *Journal of Polymer Science*, 28:631–633, 1958.

R J Ketz, R K Prudhomme, and W W Graessley. Rheology of concentrated microgel solutions. *Rheol. Acta*, 27(5):531–539, 1988.

S A Khan, C A Schnepper, and R C Armstrong. Foam rheology. 3: Measurement of shear-flow properties. *J. Rheol.*, 32(1):69–92, 1988.

W Kob and J L Barrat. Aging effects in a Lennard-Jones glass. *Physical Review Letters*, 78(24):4581–4584, 1997.

M B Kossuth, D C Morse, and F S Bates. Viscoelastic behavior of cubic phases in block copolymer melts. *Journal of Rheology*, 43:167–196, 1999.

J Kurchan. Rheology, and how to stop aging. 1998. Preprint cond-mat/9812347. To be published in proceedings of *Jamming and Rheology: constrained dynamics on microscopic and macroscopic scales* (workshop at ITP, Santa Barbara, 1997).

R G Larson. *The Structure and Rheology of Complex Fluids.* Oxford University Press, Oxford, 1999.

M R Mackley, R T J Marshall, J B A F Smeulders, and F D Zhao. The rheological characterization of polymeric and colloidal fluids. *Chem. Engin. Sci.*, 49(16): 2551–2565, 1994.

T G Mason, J Bibette, and D A Weitz. Elasticity of compressed emulsions. *Phys. Rev. Lett.*, 75(10):2051–2054, 1995.

T G Mason and D A Weitz. Linear viscoelasticity of colloidal hard-sphere suspensions near the glass-transition. *Phys. Rev. Lett.*, 75(14):2770–2773, 1995.

C Monthus and J P Bouchaud. Models of traps and glass phenomenology. *J. Phys. A*, 29(14):3847–3869, 1996.

O S Narayanaswamy. Model of structural relaxation in a glass. *J. Am. Cer. Soc.*, 54:491–498, 1971.

T Odagaki. Glass-transition singularities. *Phys. Rev. Lett.*, 75(20):3701–3704, 1995.

P Panizza, D Roux, V Vuillaume, C Y D Lu, and M E Cates. Viscoelasticity of the onion phase. *Langmuir*, 12(2):248–252, 1996.

W H Press, S A Teukolsky, W T Vetterling, and B P Flannery. *Numerical Recipes in C (2nd ed.).* Cambridge University Press, Cambridge, 1992.

G W Scherer. *Relaxation in Glass and composites.* Wiley, New York, 1986.

P Sollich. Rheological constitutive equation for a model of soft glassy materials. *Phys. Rev. E*, 58:738–759, 1998.

P Sollich, F Lequeux, P Hébraud, and M E Cates. Rheology of soft glassy materials. *Phys. Rev. Lett.*, 78:2020–2023, 1997.

L C E Struik. *Physical aging in amorphous polymers and other materials.* Elsevier, Houston, 1978.